



HAL
open science

Eruption type probability and eruption source parameters at Cotopaxi and Guagua Pichincha volcanoes (Ecuador) with uncertainty quantification

Alessandro Tadini, Olivier Roche, Pablo Samaniego, Nourddine Azzaoui, Andrea Bevilacqua, Arnaud Guillin, Mathieu Gouhier, Benjamin Bernard, Willy Aspinall, Silvana Hidalgo, et al.

► To cite this version:

Alessandro Tadini, Olivier Roche, Pablo Samaniego, Nourddine Azzaoui, Andrea Bevilacqua, et al.. Eruption type probability and eruption source parameters at Cotopaxi and Guagua Pichincha volcanoes (Ecuador) with uncertainty quantification. *Bulletin of Volcanology*, 2021, 83 (5), 10.1007/s00445-021-01458-z . hal-03208239

HAL Id: hal-03208239

<https://uca.hal.science/hal-03208239v1>

Submitted on 27 Apr 2021

HAL is a multi-disciplinary open access archive for the deposit and dissemination of scientific research documents, whether they are published or not. The documents may come from teaching and research institutions in France or abroad, or from public or private research centers.

L'archive ouverte pluridisciplinaire **HAL**, est destinée au dépôt et à la diffusion de documents scientifiques de niveau recherche, publiés ou non, émanant des établissements d'enseignement et de recherche français ou étrangers, des laboratoires publics ou privés.

[Click here to view linked References](#)

1 Eruption type probability and eruption source parameters at Cotopaxi and 2 Guagua Pichincha volcanoes (Ecuador) with uncertainty quantification

3
4 A. Tadini¹, O. Roche¹, P. Samaniego^{1,2}, N. Azzaoui³, A. Bevilacqua⁴, A. Guillin³, M. Gouhier¹, B.
5 Bernard², W. Aspinall⁵, S. Hidalgo², J. Eychenne¹, M. de' Michieli Vitturi⁴, A. Neri⁴, R. Cioni⁶, M.
6 Pistolesi⁷, E. Gaunt², S. Vallejo², M. Encalada², H. Yepes², A. Proaño², M. Pique^{2,8}

7 ¹Université Clermont Auvergne, Laboratoire Magmas et Volcans, CNRS, IRD, OPGC, 6 Avenue Blaise Pascal,
8 63178 Aubière, France.

9 ²Escuela Politécnica Nacional, Instituto Geofísico, Ladrón de Guevara E11-253 y Andalucía, Quito, Ecuador.

10 ³Université Clermont Auvergne, Laboratoire de Mathématiques Blaise Pascal, CNRS, 3 place Vasarely, 63178
11 Aubière, France.

12 ⁴Istituto Nazionale di Geofisica e Vulcanologia, Sezione di Pisa, via Cesare Battisti 53, 56125 Pisa, Italy.

13 ⁵School of Earth Sciences, University of Bristol, Wills Memorial Building, Queens Road, Bristol, BS8 1RJ,
14 United Kingdom.

15 ⁶Università degli studi di Firenze, Dipartimento di scienze della Terra, Via La Pira 4, 50121 Firenze, Italy.

16 ⁷Università degli Studi di Pisa, Dipartimento di Scienze della Terra, Via Santa Maria 53, 56126 Pisa, Italy.

17 ⁸University of Queensland, School of Earth and Environmental Sciences, St Lucia 4072, Brisbane, Australia

18
19 Corresponding author: Alessandro Tadini (Alessandro.TADINI@uca.fr)

20
21

22

23 ORCID IDs

24

25 Alessandro Tadini : 0000-0003-3603-0853

26 Olivier Roche: 0000-0002-6751-6904

27 Pablo Samaniego: 0000-0003-1169-3503

28 Andrea Bevilacqua : 0000-0002-0724-2593

29 Benjamin Bernard: 0000-0002-0333-5493

30 Willy Aspinall: 0000-0001-6014-6042

31 Silvana Hidalgo: 0000-0001-6386-9502

32 Julia Eychenne: 0000-0003-0344-6983

33 Mattia de' Michieli Vitturi: 0000-0002-6750-9245

34 Augusto Neri : 0000-0002-3536-3624

35 Raffaello Cioni : 0000-0002-2526-9095

36 Marco Pistolesi: 0000-0002-5096-3708

37 Elizabeth Gaunt: 0000-0002-1787-2062

38 Hugo Yepes: 0000-0001-6531-6311

39

40

41

42

43

44

45

46

47

48

49 **Acknowledgements**

50 The authors are grateful to Geoffrey Wadge for useful comments and advices in the early stages of this project.
51 Two anonymous reviewers are acknowledged for providing detailed comments that improved significantly the
52 quality of this paper. We also thank the editorial handling of Andrea Cannata.

53 **Funding**

54 This research was financed by the French government IDEX-ISITE initiative 16-IDEX-0001 (CAP 20-25), the
55 French Research Institute for Sustainable Development (IRD) in the context of the Laboratoire Mixte
56 International “Séismes et Volcans dans les Andes du Nord”, and the CNRS Tellus program. This work was also
57 partly funded by the ClerVolc project - Program 1 “Detection and characterization of volcanic plumes and ash
58 clouds” funded by the French government ‘Laboratory of Excellence’ initiative. This is ClerVolc contribution
59 n°477.

60 **Competing interests**

61 The authors have no competing interests to declare.

62 **Code and data availability**

63 The EXCALIBUR code used to process the data is downloadable at the following address
64 <http://www.lighttwist.net/wp/excalibur>. Other scripts to process the data are available under request – i.e. ERF
65 scores, logic tree probability calculations, Monte Carlo sampling. The raw data used in this study are available as
66 supplementary material and in a repository from the Figshare community with the following DOI
67 10.6084/m9.figshare.13148753.

68 **Authors’ contributions**

69 **A. Tadini**: Conceptualization, Formal Analysis, Investigation, Data Curation, Writing - Original Draft, Writing –
70 Review and Editing, Visualization; **O. Roche**: Conceptualization, Investigation, Writing – Review and Editing,
71 Project administration, Funding acquisition; **P. Samaniego**: Conceptualization, Investigation, Resources,
72 Writing – Review and Editing, Visualization, Supervision; **N. Azzaoui**: Conceptualization, Investigation,
73 Writing – Review and Editing, Visualization, Supervision; **A. Bevilacqua**: Formal Analysis, Software,
74 Investigation, Data Curation, Writing – Review and Editing, Visualization; **A. Guillin**: Conceptualization,
75 Investigation, Writing – Review and Editing, Project Administration, Supervision, Funding Acquisition; **M.**
76 **Gouhier**: Conceptualization, Investigation, Writing – Reviewing and Editing, Supervision; **B. Bernard**:
77 Investigation, Resources, Writing – Review and Editing, Funding Acquisition; **W. Aspinall**: Methodology,
78 Software, Investigation, Writing – Review and Editing, Visualization; **S. Hidalgo**: Investigation, Resources,
79 Writing – Review and Editing, Visualization; **M. de’Michieli Vitturi**, **A. Neri**, **R. Cioni**, **M. Pistolesi**, **E.**
80 **Gaunt**, **S. Vallejo**, **M. Encalada**, **H. Yepes**, **A. Proaño**, **M. Pique**: Investigation, Writing – Review and
81 Editing.

82 **Abstract**

83 **Abstract**
84 Future occurrence of explosive eruptive activity at Cotopaxi and Guagua Pichincha volcanoes, Ecuador, is
85 assessed probabilistically, utilizing expert elicitation. Eight eruption types were considered for each volcano.
86 Type event probabilities were evaluated for the next eruption at each volcano and for at least one of each type
87 within the next 100 years. For each type, we elicited relevant eruption source parameters (duration, average
88 plume height and total tephra mass). We investigated the robustness of these elicited evaluations by deriving
89 probability uncertainties using three expert scoring methods. For Cotopaxi, we considered both rhyolitic and
90 andesitic magmas. Elicitation findings indicate that the most probable next eruption type is an andesitic
91 hydrovolcanic/ash-emission (~26-44% median probability), which has also the highest median probability of
92 recurring over the next 100 years. However, for the next eruption at Cotopaxi, the average joint probabilities for
93 sub-Plinian or Plinian type eruption is of order 30-40% - a significant chance of a violent explosive event. It is
94 inferred that any Cotopaxi rhyolitic eruption could involve a longer duration and greater erupted mass than an
95 andesitic event, likely producing a prolonged emergency. For Guagua Pichincha, future eruption types are
96 expected to be andesitic/dacitic, and a vulcanian event is judged most probable for the next eruption (median
97 probability ~40–55%); this type is expected to be most frequent over the next 100 years, too. However, there is a
98 substantial probability (possibly >40% in average) that the next eruption could be sub-Plinian or Plinian, with all
99 that implies for hazard levels.

100

101 **Keywords**: Cotopaxi volcano, Guagua Pichincha volcano, volcanic hazard, elicitation, uncertainty
102 quantification

103

104 1. Introduction

105
106 The future behavior of a volcano is a matter of central concern for volcanic hazard and risk assessment. The
107 estimation of probability of eruption scenarios depends on two factors: i) the temporal probability of an eruption
108 and ii) the conditional probability of a particular eruptive scenario given that an eruption occurs (Connor et al.
109 2015; Poland and Anderson 2020). In this study we will mostly focus on the latter. These probabilities serve as a
110 basis for scenario and evacuation plan definition, long-term urban planning and risk mitigation. Additionally, the
111 estimate of the uncertainty ranges for eruption source parameters (ESPs) is a key aspect for the development of
112 probabilistic hazard maps, which mainly rely on numerical models (e.g., Costa et al. 2009; Bonasia et al. 2011;
113 Biass et al. 2014; Vázquez et al. 2019). To the extent that the past eruptive history of a volcano is known and
114 rigorously analysed, both aspects can be addressed with some measure of accuracy provided associated
115 uncertainties are accounted for.

116 While the recurrence probabilities of different volcanic eruptions can be assessed through the development
117 of temporal models (e.g., Mulargia et al. 1985; De la Cruz-Reyna 1993; Bebbington and Cronin 2011;
118 Bevilacqua et al. 2016), conditional probabilities of eruption type are usually described using either Bayesian
119 belief networks (e.g., Aspinall and Woo 2014; Hincks et al. 2014; Christophersen et al. 2018) or event trees (e.g.,
120 Newhall and Hoblitt 2002; Martí et al. 2008; Neri et al. 2008; Tierz et al. 2020). Incompleteness and uncertainty
121 of the eruptive records affect temporal modelling, and difficulties in incorporating monitoring signals are
122 challenging issues that have been tackled using several approaches, including hidden Markov models (Aspinall
123 et al. 2006; Wang and Bebbington 2012; Bevilacqua et al. 2020a), variably combined statistical models
124 (Marzocchi and Bebbington 2012; Runge et al. 2014; Bevilacqua et al. 2018) or the failure forecast method
125 (Voight 1988; Robertson and Kilburn 2016; Kilburn 2018; Bevilacqua et al. 2019; Bevilacqua et al. 2020b;
126 Bevilacqua et al. 2020c).

127 Each eruption of a volcano is characterized by specific ESPs whose range of variation, especially if they are
128 factors to be applied in probabilistic studies, can be estimated from field data (e.g. Macedonio et al. 2016; Parra
129 et al. 2016; Biass et al. 2017) or derived from analogue volcanoes and/or general distribution of ESPs (e.g.
130 Mastin et al. 2009; Sheldrake 2014; Sheldrake et al. 2016; Gouhier et al. 2019). While it is straightforward to
131 define a uniform probability distribution between two end-member values for each ESP, this approach can entail
132 potential loss of information that might be present in data and records, which may provide an objective basis for
133 a more informative uncertainty distribution function. To offset such limitations, it can be useful to adopt
134 structured expert judgment techniques (Aspinall 2006; Aspinall and Cooke 2013) to explicitly derive a unique
135 credible uncertainty range and a corresponding elemental probability distribution for each of the investigated
136 variables through weighted pooling of a group of experts' uncertainty distributions. This approach has been
137 adopted both for describing the future behavior of a volcano (Martí et al. 2008; Neri et al. 2008) and also for
138 determining some ESPs (Bebbington et al. 2018; Christophersen et al. 2018; Aspinall et al. 2019).

139 The aim of this paper is to report assessed conditional probabilities of experiencing different eruption types
140 (and their main ESPs) - conditional on the future occurrence of an eruption - at Cotopaxi and Guagua Pichincha
141 volcanoes, two of the most active and hazardous volcanoes in Ecuador. At both volcanoes, the spectrum and
142 magnitudes of potential eruptive types can range from minor but long-lasting ash emissions or vulcanian to
143 Plinian eruptions, and their relative probabilities of occurrence must be assessed on a coherent basis to obtain
144 self-consistent volcanic hazards assessments and to support reasoned decision-making. In this paper we are
145 focusing on explosive eruptions due to the greater hazard that they pose in terms of the large areas potentially
146 affected by tephra dispersal.

147 Here, these challenges are addressed with an established expert elicitation methodology for the formal
148 numerical quantification of uncertainties, the results of which can inform event trees for the two volcanoes.
149 These findings contribute to a long-term project aimed at developing new probabilistic tephra hazard maps for
150 Cotopaxi and Guagua Pichincha volcanoes. In this project, a new procedure for quantifying relevant
151 uncertainties in a tephra transport and dispersal model has been recently proposed (Tadini et al. 2020). Here, the
152 quantification of other, related uncertainties (both epistemic and aleatoric, Tadini et al. 2017b) represents a
153 further advance towards a fully probabilistic volcanic hazard assessment approach that will enable uncertainties
154 to be explicitly accounted for producing the resulting tephra hazard maps.

155 For Cotopaxi, two studies have been recently published about tephra fallout hazard and risk assessment.
156 Biass and Bonadonna (2013) developed semi-probabilistic and probabilistic hazard maps and curves by using the
157 TEPHRA2 model (Bonadonna et al. 2005) and considering eruptive scenarios with $VEI \geq 3$. Moreover, using
158 data from the global volcanism program database, the authors calculated the probability of occurrence of an
159 eruption of $VEI \geq 3$ for the next 10 (36.2%) and 100 (98.9%) years. Additionally, Biass et al. (2013) performed a
160 risk assessment for eruptions with $VEI \geq 4$, highlighting the possible collapse due to ash loading of several
161 thousands of houses in the proximity of the volcano, the destruction of agriculture and the possible disruption of
162 major roads. The potential high impact of tephra fallout on the new Quito International airport, considering
163 Cotopaxi among other volcanoes, has been addressed by Volentik and Houghton (2015). For Guagua Pichincha,

164 they highlighted that the small-size AD 1999 eruption (see section 2.2) resulted in huge economic losses to the
165 tourism and agricultural sectors. In order to consider further the impact that an eruption of even moderate size
166 could have on aviation, the definitions of eruptive scenarios and recurrence probabilities for Cotopaxi and
167 Guagua Pichincha are therefore crucial.

168 Before addressing these and other hazard-related assessment issues, we provide first a general overview on
169 Cotopaxi and Guagua Pichincha volcanoes (section 2) and on expert elicitation techniques (section 3, with
170 details in the Appendix). Then, we present a detailed analysis of our findings (section 4), with further
171 considerations about the procedure and prospective implications for hazard levels at Cotopaxi and Guagua
172 Pichincha (section 5).

173 2. Volcanic context

174
175 Cotopaxi and Guagua Pichincha volcanoes (Fig. 1) are located, respectively, ~60 km South and ~10 km
176 West of Quito, Ecuador's capital city. About 150,000 and 2 million inhabitants live within 30 km of Cotopaxi
177 and Guagua Pichincha volcanoes (Global Volcanism Program 2013), respectively.

179 2.1 Cotopaxi volcano

180 Cotopaxi is a 5,897 m high active volcano located on the Eastern Cordillera. According to Hall and Mothes
181 (2008), the eruptive history of Cotopaxi volcano started roughly 0.5 Ma, and it is characterized by a bimodal
182 volcanism involving rhyolitic (70–75 wt.% SiO₂) and andesitic (56–62 wt.% SiO₂) magmas. The same authors
183 calculated a total erupted DRE volume during the last 0.5 Ma of 28.54 km³ and they gave a detailed evolution of
184 total erupted volume with time (Fig. 20 of Hall and Mothes 2008). Cotopaxi activity was characterized during its
185 early stages by a series of large eruptions involving magmas of rhyolitic composition lasting ~0.1 Ma (Barrancas
186 series, Hall and Mothes 2008). After a long repose period of ~0.4 Ma, except for a short andesitic activity at
187 around 0.45 Ma BP (Rio Pita Series), the volcanic activity resumed with other five eruptive episodes (F series,
188 Hall and Mothes 2008). Such series (9.6–5.5 ka BP) were mainly rhyolitic in composition, but andesitic magmas
189 erupted repeatedly, a fact that allowed Hall and Mothes (2008) to infer that andesitic magma already existed or
190 was rising from depth. The subsequent Colorado Canyon series (~4.5 ka) involved rhyolitic magmas and
191 included a sector collapse on the NE side of Cotopaxi (Smyth and Clapperton 1986; Mothes et al. 1998; Vezzoli
192 et al. 2017). From the end of the Colorado Canyon episode until the present day, magmas erupted from Cotopaxi
193 were almost all andesitic in composition, except one rhyolitic ash level dated at 2.1 ka (Barberi et al. 1995; Hall
194 and Mothes 2008). For the period 4–1 ka, Hall and Mothes (2008) reported a total of 25 eruptions (18 of which
195 were considered as Plinian events with VEI 4). The subsequent period represented the historical activity of
196 Cotopaxi volcano, which lasted from AD 1532–34 up to AD 1880, with minor activity occurring in the 20th
197 century (Pistolesi et al. 2011) and a full resumption of activity with the AD 2015 eruption (Bernard et al. 2016;
198 Hidalgo et al. 2018). The period 1532–1880 (total erupted volume of 2.14 DRE km³, Hall and Mothes 2008) was
199 studied in detail by Pistolesi et al. (2011) who identified 13 layers/eruptions grouped in 6 sets. Within the last 1
200 ky, all the eruptions involved andesitic magmas and there have been both violent Strombolian VEI 2–3 (AD
201 1853), sub-Plinian VEI 3–4 (AD 1877 and XVIII century) and Plinian VEI 4–5 (Layer 3 - 820±80 years BP;
202 Layer 5 - 1180± 80 years BP, Biass and Bonadonna 2011; Tsunematsu and Bonadonna 2015) eruptions. After
203 small-scale (VEI 1–2) explosions reported in the years 1904 and 1942 (Pistolesi et al. 2011), Cotopaxi
204 reawakened in AD 2015 resulting in a ~3 months long eruption, characterized by an opening hydrovolcanic (or
205 phreatomagmatic) phase (Bernard et al. 2016) followed by a long-lasting ash emission (Gaunt et al. 2016;
206 Hidalgo et al. 2018). Table 1 summarizes the main typologies of explosive eruptions of Cotopaxi considered in
207 the production of the logic trees in the following sections. We highlight that this table does not record completely
208 the eruptive history of the volcano, but it has been used as a basis to describe the spectrum of explosive activity
209 at Cotopaxi volcano. Despite this explosive activity is preponderant, effusive activity at Cotopaxi is also
210 documented (Hall and Mothes 2008; Pistolesi et al. 2011), although it is often linked to other explosive eruptions
211 (e.g. AD 1853; Pistolesi et al. 2011). For this reason, a separate category of “effusive eruption” has not been
212 considered in our study.

214 2.2 Guagua Pichincha volcano

215 The Pichincha volcanic complex is composed of two distinct edifices sitting atop the El Cinto lavas (0.1–1.1
216 Ma, Robin et al. 2010), the older Rucu Pichincha (4,694 m a.s.l.) and the younger Guagua Pichincha (4,784 m
217 a.s.l.). The magmatic composition of the erupted products of both the Rucu and Guagua Pichincha is andesitic to
218 dacitic (55–66 wt.% SiO₂), while the eruptive history of the former spans the period 0.85 Ma–0.15 Ma and the
219 second began to erupt at around 60 ka (Robin et al. 2010). The development of the Guagua Pichincha volcano

220 involved two major sector collapses (at ~11 ka and ~4 ka), which were linked to changes in the erupted rock
221 chemistry due to the arrival of new magma batches (Robin et al. 2010). The last “Toaza” sector collapse
222 occurred around 4 ka and the volcanic activity resumed roughly 2 ka with the development of a new summit
223 dome (the “Cristal dome”). This dome experienced phases of growth /collapse and related block-and-ash flows
224 and blasts (Robin et al. 2008). Due to the above-mentioned changes in rock chemistry that occurred after the
225 “Toaza” sector collapse, we will focus on the eruptive history after 4 ka. The volcanic activity of the last 2000
226 years has been the topic of several studies aimed at better characterizing the stratigraphy, the chronology of the
227 eruptions and the volcanic hazard (Geotermica Italiana 1989; Barberi et al. 1992; Robin et al. 2008). This period
228 involved three major eruptive cycles (I century, X century, Historic) separated by repose periods of the order of
229 300–500 years. Each cycle was initiated with phases of dome emplacement and explosive episodes, and involved
230 a final Plinian-like eruption (Robin et al. 2008). As a reference, the Historic cycle involved at least 3 eruptive
231 explosive episodes (testified by historical accounts, Wolf 1904) in AD 1566, 1575, and 1582, with ash fallout in
232 Quito and pyroclastic density currents at the west side of the volcano. The Plinian-like eruption of AD 1660
233 closed this cycle (Robin et al. 2008). After the Historic cycle, phreatic explosions occurred at Guagua Pichincha
234 in the XIX century and became more frequent (and correlated with seasonal rain) in the years 1981-1998
235 (Garcia-Aristizabal et al. 2007). Particularly, in AD 1998 there was a sudden increase of the phreatic activity,
236 which presaged the first dome-forming eruption of the 1999-2001 cycle. During this cycle, 8 dome-forming
237 eruptions (each of them followed by the dismantling of the newly formed dome) took place, and several
238 Vulcanian eruptions (including the AD 1999, the largest of the cycle) destroyed the first domes (Garcia-
239 Aristizabal et al. 2007; Wright et al. 2007). The similarities (in terms of eruptive styles) between the eruptive
240 cycle of 1999-2001 with the early stages of the Historic and X century cycles, permitted Robin et al. (2008) to
241 infer that the 1999-2001 cycle might be the first step of a mid-term evolution that will eventually result in a
242 Plinian-like eruption like that of AD 1660. Table 2 summarizes the main typologies of explosive eruptions of
243 Guagua Pichincha volcano considered in the production of the logic trees in the following sections. Also in this
244 case we report in this table just a selection of eruptions to define the typologies for the logic trees in Fig. 2. For
245 Guagua Pichincha, differently from Cotopaxi, the effusive dome-forming activity is more significant, but it is not
246 considered in our study due to the specific focus on explosive activity.
247

248 **3. Methods**

249

250 *3.1 Elicitation*

251 Our study involved all the participants in the author list, representing different levels of experience and
252 a variety of scientific backgrounds. These specialists all have at least a basic background in volcanology, and the
253 majority has undertaken detailed work on Cotopaxi or Guagua Pichincha volcanoes, or both. The elicitation (see
254 Appendix A for details) started with a seed questionnaire (for determining experts’ weighting) composed of 15
255 factual questions about Ecuadorian/South American volcanism and numerical modelling of volcanic ash
256 (without considering monitoring data). Participants were not expected to know precisely the quantitative values
257 of the questions but they were expected to be able to provide credible intervals that captured the ‘true’ values for
258 at least some of the questions. Thus, for each question, participants were asked to provide their immediate
259 uncertainty judgments by suggesting their own 5th percentile, 50th percentile (median), and 95th percentile
260 estimates of the – for them, unknown - values in question. To avoid influencing and group-thinking, each person
261 responded individually and confidentially to the elicitation facilitator. The seed questionnaire used in this session
262 is provided as Online Resource 1.

263 These questions were processed by applying three well-established scoring methods to calculate each
264 expert’s calibration and informativeness scores (details are available in the Appendix A). The methods are
265 Cooke’s Classical Model (CM - Cooke 1991; Aspinall 2006), the Expected Relative Frequency method (ERF -
266 Flandoli et al. 2011; Bevilacqua 2016), and the Equal Weights (EW) rule (Bevilacqua 2016). The purpose of
267 using three scoring methods is twofold. First, it underlines the robustness of the outcomes where CM, ERF and
268 EW methods have similar or coincident trends. Second, it can help identifying if two or more different “school
269 of thoughts” exist among the experts on any item of interest. A discussion about the outcomes of the three
270 scoring methods (CM, ERF and EW) is given in Flandoli et al. (2011) and reported in Appendix A.

271 The calibration and informativeness scores are thus used to define each expert’s weight to be applied when
272 considering the judgments on the ‘target item’ questions, i.e. the variables of interest. In this form, target item
273 responses are pooled together with the experts’ weights to produce a group synthesized uncertainty distribution,
274 often called a ‘decision maker’ solution (DM). Where necessary for clarity in the paper, we will also call
275 “decision-taker” the actual person in charge of taking decisions. As with the calibration questions, for the target
276 questions the experts were asked again to provide their judgments and associated uncertainties as 5th percentile,
277 50th percentile (median), and 95th percentile values. The advantage of this approach (especially for ESPs) is that

278 it is possible to obtain elemental uncertainty distribution markers for each variable and not just simple variation
279 ranges between a maximum and minimum value.

280 The purpose of the target questionnaires about Cotopaxi and Guagua Pichincha was twofold. Firstly, it
281 aimed at assessing the relative conditional probability of different types of volcanic activity (see Appendix A for
282 the definition of “eruption” used in this study) and associated magma composition (the latter for Cotopaxi only)
283 in a specific temporal frame. More specifically, such questions were considered in two frameworks, namely the
284 “next eruption” and the “next 100 years” cases, the former being the most explosive phase of the eruption
285 considered and the latter being the probability of having at least one eruption type/magma composition within
286 the next 100 years. We introduced this differentiation because the ‘next eruption’ case is surely the most relevant
287 for short to medium-term hazard assessment, but that would have to be updated with new expert judgments and
288 re-evaluated after a new eruption would occur. On the contrary, the ‘next 100 years’ case aims at providing a
289 longer time frame and it facilitated the experts in focusing on single eruptions in such time frame. These two sets
290 of questions are denoted, respectively, with the abbreviations “NE” and “N100” in the following sections. An
291 important consequence of this subdivision is that, while the NE case contains mutually exclusive events
292 summing to 100%, the N100 case does not exclude the possibility of having eruptions of different type as
293 subsequent events.

294 Figure 2 displays the logic tree for Cotopaxi and Guagua Pichincha, whose branches represent the above-
295 mentioned target questions. With these event trees we aim at quantifying the conditional probability of explosive
296 eruptions, as they pose a higher number of hazards than effusive ones. The latter should be considered as part of
297 the “Other eruption” types, which include both effusive events and other events not recorded in the stratigraphy
298 of the volcano nor in the historical observations. However, we do not exclude that for some other type of
299 eruptions (for example the “Violent Strombolian” or “Vulcanian” for Cotopaxi and Guagua Pichincha,
300 respectively) there may be some lava outpourings associated to the eruption scenario.

301 The probability of occurrence of the various types of volcanic activity could be also inferred from the
302 available information on past recurrence rates in the global datasets of volcanic eruptions (Smithsonian GVP,
303 LaMEVE). Statistical modeling of global VEI-frequency distributions using extreme value methods (Coles and
304 Sparks 2006; Deligne et al. 2010; Furlan 2010; Rougier et al. 2016; Papale 2018), or through comparison of the
305 global record with the well-characterized record in Japan (Kiyosugi et al. 2015) provide insight into possible
306 corrected distributions, but regional differences make the global record difficult to apply to single volcanoes
307 (Rougier et al. 2018). Much remains to be learned about global trends in volcanic explosivity, and uncertainty is
308 very high (Deligne et al. 2017). In particular, there are problems with calculation of VEI distribution through
309 time, including under-recording of small magnitude events backward through time, and over-recording of VEI 2
310 events by the Smithsonian GVP. For these latter reasons, our expert judgment approach does not rely on such
311 global data.

312 The target questionnaires addressed also the uncertainty range of some key ESPs (eruption duration in
313 minutes, total mass of the tephra fallout deposit in 10^9 kg and average plume height in km) for the different types
314 of eruptions, according their importance for volcanic hazard assessment and numerical modelling, especially
315 concerning tephra fallout.

316 We have not directly elicited some other parameters important for tephra fallout hazard assessment and
317 numerical modeling, such as total grain-size distribution, particle densities, particle shape factors, and initial
318 volatile content of magma. For these parameters we have considered that either their uncertainty has been
319 already adequately modeled without using expert judgment techniques (e.g. total grain-size distribution, Costa et
320 al. 2016) or that their uncertainty range might be better described by a linear variation between two end-
321 members. For example, in this latter case, we found good constraints for both Cotopaxi and Guagua Pichincha
322 volcanoes for initial water mass fractions (Wright et al. 2007; Samaniego et al. 2010; Andújar et al. 2017; Martel
323 et al. 2018), particle densities (Bonadonna and Phillips 2003; Pistolesi et al. 2011) and particle shape factors
324 (Riley et al. 2003).

325 4. Results

326

327 4.1 Eruption probabilities and ESPs

328 In this section, we report the results of the elicitation, subdivided in graphical outputs (Figs. 3 and 4) and
329 triplets of values (Tables 3-6). The graphical outputs show the probability density functions of the DM resulting
330 from the application of a Gaussian kernel density estimator (Silverman 1986; Connor and Connor 2009; Tadini
331 et al. 2017a) to the weighted combination of the experts’ probability distribution judgments. This means that we
332 extracted a sufficient number of samples (10^5) of expert answers, a number selected by iteration to assure a
333 robust convergence of the kernel density estimator. This differs from the original formulation of the ERF method
334 (Flandoli et al. 2011), in which the DM resulted from the linear combination of the quantiles of the experts’
335 probability distributions. In particular, we abandoned the quantile combination approach because it would have

336 averaged the median values of different experts instead of producing multimodal distributions (e.g. Bevilacqua,
337 2016). More specifically, when calculating the DMs, we performed a linear combination (i.e. a probability
338 mixture) of maximum entropy distributions, i.e. uniformly distributed between the elicited percentiles (Cooke,
339 1991) in all the three methods. We remark that in the calculation of the ERF scores on the ‘seed questionnaire’
340 we adopted triangular probability distributions, while for the definition of the DM on the ‘target questionnaire’
341 we used maximum entropy distributions. This choice enabled a better comparison of ERF with the CM and EW,
342 but it differs from Bevilacqua et al. (2015) and Tadini et al. (2017a).

343 We also highlight that multi- or bimodality in the resulting probability density functions is a consequence
344 of the different modes expressed by different experts, while the full uncertainty range (in Tables 3-6) is obtained
345 from the envelope of all experts and their judgments. The triplets of values in the tables therefore summarize the
346 DM’s probability distribution with three percentiles (5th, 50th and 95th). These triplets have been recalculated
347 from the original elicitation data in order to have conditional probabilities with respect to rhyolitic or andesitic
348 magmas, respectively. Given the large amount of elicitation data, we only report in the main text the graphical
349 outputs of the conditional probabilities. Those of the ESPs are provided in the supplementary material (Online
350 resource 2), together with the experts’ weights (Online resource 3).

351 For Cotopaxi volcano, the results of the elicitation are provided in Figure 3, Table 3 (conditional
352 probabilities) and Table 5 (ESPs) for the CM, ERF and EW methods. Similarly, for Guagua Pichincha volcano,
353 results are provided in Figure 4, Table 4 (conditional probabilities) and Table 6 (ESPs). Eruption durations are
354 given in minutes. We highlight two general observations. Firstly, for all the distributions, in our formulation, the
355 ERF answers are generally between the CM and the EW ones, and they are significantly closer to the latter; this
356 is particularly evident by comparing the probability density functions (see Figs. 3 and 4). Secondly, if the
357 uncertainty range of the distributions is considered (i.e. the 5th and 95th percentiles in Tables 3, 4, 5 and 6), the
358 CM distributions are in general more informative, that is, they are more focused (although slightly) around the
359 50th percentile.

360 For Cotopaxi, considering the CM method, we evaluated that the three percentiles (5th, 50th, 95th) of the
361 conditional probability that the next eruption (NE case) will involve rhyolitic magma are [0.4, 8.4, 39] %, with a
362 mean value of 13%. The ERF and EW methods produced median values of 11 - 12% and mean values of 16 -
363 20%. In contrast, the conditional probability of having eruptions involving andesitic magmas is [61, 92, >99] %,
364 with a mean value of 87% considering the CM method. In these two cases, the corresponding probability density
365 functions for all the scoring methods (Fig. 3) show a clear unimodality, with the CM scoring method having a
366 slightly higher peak with respect to ERF and EW. Instead, in the rhyolitic case, the probability density functions
367 for the sub-Plinian and Plinian eruptions are markedly multimodal for all the scoring methods, with the ERF and
368 EW solutions having similar trends. The different probability peaks are illustrated in Figure 3. In the andesitic
369 case, the hydrovolcanic/continuous ash emission (like AD 2015) has been evaluated the most probable next
370 eruption (NE case). There are, however, some differences among the scoring methods, with the ERF and the EW
371 having noticeably lower median values (28% and 26%) than the CM solution (44%) – (mean values of 28%,
372 27%, and 44% respectively). Similar inferences can be made for the corresponding probabilities in the N100
373 case at Cotopaxi, with probability values that are generally higher because we did not assume mutually exclusive
374 events. For example, the median probability of at least one hydrovolcanic/continuous ash emission in the next
375 100 years is 43 - 55%, depending on the method (mean values in 43 - 51%). We remark that the above-
376 mentioned cases for the NE case, where distributions show bi- or multimodality, have bi- or multimodality also
377 in the N100 case, with even more fluctuations (see Fig. 3).

378 For the NE case at Guagua Pichincha, despite the fewer number of eruption types (and just one magma
379 composition in consideration), there is one eruption type (i.e. Vulcanian – see Table 4 and Fig. 4) for which there
380 are relatively large differences among the scoring methods. A Vulcanian eruption has been considered the most
381 probable event, but the median values are 55% for the CM, 45% for the ERF and 40% for the EW (mean values
382 of 51%, 44%, and 40%). More details about the other percentiles can be found in Table 4 and in Appendix B.
383 The differences among the three scoring methods is, in contrast, lower for the other cases (sub-Plinian, Plinian
384 and other – Fig. 4). We remark also that the median conditional probability for “Other” eruption types has been
385 evaluated with a median probability ranging from 7.5% up to 11%, depending on the method selected (mean
386 values of 13% up to 18%). For the N100 case, considerations similar to those for Cotopaxi can be made as there
387 are larger fluctuations in the probability density functions (Fig. 4), describing bi- or multimodal distributions for
388 all cases (except for the “Other eruption” case).

389 Considering parameter uncertainty ranges for both Cotopaxi and Guagua Pichincha (Tables 5 and 6), the
390 average plume height is the parameter for which the differences among the three scoring methods are lowest (see
391 also Online resource 2). In general, however, differences between the median values of the other two parameters
392 (total mass and total duration) for the three scoring methods are generally low.

393 4.2 Sensitivity of variable weights to expert group composition

394 Three sensitivity assessments of the outcomes of the CM analysis were performed with respect to experts'
395 career ages, main scientific expertise and geographic affiliation at the time of the elicitation. The goal was to
396 highlight possible trends that might have been influenced by the different backgrounds/experiences of the
397 various experts involved. It is important to highlight that, with respect to any of the sub-groups, the CM
398 outcomes are not a measure of the average knowledge of the participants of a sub-group about the volcanological
399 problem as a whole, but rather a measure of the participants' abilities to judge volcanological quantitative
400 uncertainties. Weights assigned with the EW rule are reported as well in order to highlight the overall agreement
401 or disagreement among experts within different sub-groups. Six sub-groups were analyzed as paired
402 comparisons, which are: Senior researchers vs. Early-career researchers (A1 vs. A2 – 14 and 6 experts
403 respectively); Geologists vs. Mathematicians-Modelers (B1 vs. B2 – 9 and 11 experts respectively) and
404 Clermont-Ferrand vs. Quito (C1 vs. C2 – 12 and 8 experts respectively). The latter group refers to the location of
405 the experts at the time of the elicitation, which was performed in one single session, but with experts remotely
406 connected from the two different localities. Senior researchers were those with > 10 years of academic career
407 after obtaining the PhD. The pairs of sub-groups (e.g. A1/A2 vs. B1/B2) are significantly different and not
408 correlated by construction. Therefore, the elicitation responses have been analyzed in order to highlight possible
409 biases given by the fact that, within the sub-group C1, some experts have not worked on the studied volcanoes as
410 deeply as those of sub-group C2. The complete dataset for this analysis is available in Online resources 6 and 7.

411 To compare the outputs of the elicitation considering the whole group or different sub-groups, we have
412 analyzed the outputs in the two tables in Supporting Information by performing principal component analysis
413 (PCA) of the data (Wold et al. 1987; Chiasera and Cortés 2011). This procedure allowed us to obtain the PCA
414 eigenvector and its eigenvalues (described by two dimensions' x and y referred here as Dim1 and Dim2), which
415 indicate the direction of maximum spread of multivariate data. As shown in Figure 5, we used CM data to create
416 sub-plots with normalized eigenvectors for two sub-groups (A1 vs. A2, B1 vs. B2, C1 vs. C2), along with that of
417 the whole group (All). This approach allows us to discuss, for each sub-plot, how similar the absolute values,
418 obtained considering the group as a whole (All), are to one sub-group or another.

419 We remark that in Fig. 5 the direction of each arrow could vary as a function of the uncertainty spread of
420 the DM solution for each subgroup, and that if the arrow of one subgroup is closer to the reference "All" arrow,
421 this indicates that the two are more closely similar to each other than the DM solution of the other subgroup.
422 Conversely, equidistance of the "All" arrow from both subgroups indicates that the "All" DM is balanced
423 between them.

424 Results displayed in Figure 5 highlight the following trends: i) eigenvectors of the sub-groups for Cotopaxi
425 (Fig. 5a) tend to have an higher spread, within each sub-plot, than those of Guagua Pichincha (Fig. 5b), as
426 indicated by the higher percentages of Dim2 in all the Cotopaxi sub-plots; ii) eigenvectors of ESPs tend to be
427 more closely related to their corresponding "All" solutions than those of conditional probabilities for both
428 volcanoes, with the exception of sub-groups A1 vs. A2 (Senior researchers vs. Early-career researchers); iii) for
429 both volcanoes, the eigenvector representing the whole group ("All") tends to be placed in the middle of the
430 sector defined by the eigenvectors C1 vs. C2 (Clermont-Ferrand vs. Quito), while that for A1 vs. A2 (Senior
431 researchers vs. Early-career researchers) tends to be closer to the eigenvector A1 and that for B1 vs. B2
432 (Geologists vs. Mathematicians-Modelers) tends to be consistently closer to the eigenvector B1.

433 These analysis findings, and their possible implications, are discussed in more detail in Section 5 below.
434

435 5. Discussion

436

437 5.1 Expert scoring methods and sensitivity analyses

438 In this paper we provide a detailed method to analyze an elicitation that addressed future eruption types
439 and their likelihoods for Cotopaxi and Guagua Pichincha volcanoes. Our approach involves comparisons of
440 probability density functions from the experts' judgments about eruption probabilities and eruptive parameters
441 (Tables 3 and 4, Figs. 3 and 4 and Online resource 2). In earlier studies that involved comparison between
442 different scoring methods (for Campi Flegrei/Vesuvius volcanoes), consistency of elicitation outputs suggested
443 that the findings were similar among them and robust (Bevilacqua et al. 2015; Tadini et al. 2017a). In this new
444 study we find the same trend of consistency for the majority of the questions, suggesting again the general
445 robustness of elicitation outputs. In just two cases a slightly greater intrinsic uncertainty on some of the issues
446 elicited demonstrated that different results could be obtained when scoring the experts in a different way (e.g.
447 "Hydrovolcanic/Ash emission eruption – NE " for Cotopaxi, Fig. 3; "Vulcanian eruption - NE " for Guagua
448 Pichincha – Fig. 4). These differences highlight a general uncertainty in characterizing both the occurrence and
449 the ESPs of these types of small magnitude eruptions, for which there is not an extended worldwide database and
450 which might have been more frequent than those recorded in the stratigraphic record. In addition, it is also more

451 difficult to place these eruption types within well-known eruption categories, which are often mostly based on
452 larger magnitude events (see for example Mastin et al. 2009). More studies are therefore needed in this sense. It
453 is also important to remind that in this study we have used a classification scheme for eruptions that differs from
454 the classical VEI scale: this might also explain some differences observed in experts' assessments, which might
455 give different VEI scale representations within our classes. Furthermore, while not being highly relevant, the
456 highlighted differences among scoring methods could be taken into consideration if these particular outputs were
457 to be used for any hazard or risk decision purposes, and in general a choice should be made about which solution
458 to adopt: that of the CM, the ERF or the EW method. Notwithstanding the CM scoring method has been used
459 traditionally in many studies, both in volcanology and other fields (Aspinall 2006), the choice about which
460 outcome to consider is ultimately a responsibility of the (human) decision-taker. With respect to this latter issue,
461 it is worth keeping in mind that the CM is a "selective" scoring method (due to the properties of the "calibration"
462 score, see Appendix A) and is therefore efficient in selecting, from a potentially large group of experts, those that
463 are statistically more accurate in constraining uncertainties. On the other hand, a less "selective" scoring method,
464 like ERF, gave results similar to that of the EW method, if compared to the CM. This similarity was enhanced by
465 having used the same DMs definition algorithm in all the methods, except for the difference in the experts'
466 scores. While in most of the situations performing this selection using the CM scoring method is justified, in
467 other contexts it can be important for the human decision-taker to consider pooling outcomes derived from the
468 judgments of the group as a whole (i.e. by considering counterpart EW or ERF DM solutions). In summary,
469 comparing the outcomes of different scoring methods allows highlighting differences in scientific basis that
470 might influence expert forecasts. Such differences are related to variation in assessment of incompleteness of the
471 eruptive record or variations in the different models (scientific, conceptual, or mechanical) assumed by the
472 experts for providing their judgments. The investigation of the motivations behind the differences between the
473 experts responses is not the aim of the elicitation session (see Appendix A; Cooke, 1991).

474 To provide more cogency for the choice of one scoring method over another, or to select estimations
475 obtained from one specific sub-group of experts, we have also performed PCA analysis to explore the relative
476 information contents of each option. The trends discussed in section 4.2 highlight primarily that, for the two
477 volcanoes, the experts' judgments are slightly less homogeneous for Cotopaxi than for Guagua Pichincha, as
478 indicated by the higher Dim2 percentages in all the sub-plots of Figure 5a with respect to those of Figure 5b.
479 Very likely, this observation could be correlated with the higher complexity of the logic tree of Figure 3
480 (Cotopaxi) versus Figure 4 (Guagua Pichincha). In other words, the greater number of eruption types and the
481 potential involvement of two alternative different magmas complicates matters for Cotopaxi compared with
482 Guagua Pichincha.

483 Moreover, the ESP PCA sub-plots for Cotopaxi have a higher Dim2 value than that of Guagua
484 Pichincha. This could be linked to the greater difficulty in constraining uncertainty ranges for the ESPs of the
485 small magnitude eruptions as the hydrovolcanic/continuous ash emission (Bernard et al. 2016) and Violent
486 Strombolian type eruptions. However, for both volcanoes (especially for the sub-groups B1 vs. B2, and for C1
487 vs. C2) Dim2 is lower for the sub-plots with ESPs than for the corresponding sub-plots for conditional
488 probabilities, suggesting a greater uniformity of judgments among sub-groups for ESPs than for conditional
489 probabilities.

490 Finally, an important aspect is linked to the orientation of the eigenvector of the whole group (All) with
491 respect to those of the sub-groups. As highlighted in section 4.2, the eigenvector "All" is found to be located in
492 the middle of the sector defined by the alternate eigenvectors C1 vs. C2, for both Cotopaxi and Guagua
493 Pichincha. This observation indicates that the final absolute values are equally distant (and therefore balanced)
494 between the judgments of the two sub-groups with different institutional locations (i.e. Clermont-Ferrand and
495 Quito). However, for the sub-plots A1 vs. A2 and for B1 vs. B2 in Figure 5, the "All" eigenvectors are generally
496 closer to A1 (Senior Researchers), and more toward B1 (Geologists) in the latter. These findings suggest that
497 institutional affiliation did not influence the DM as much as age and background.

498 *5.2 Implications for hazard assessment and numerical modelling*

499 The results of the elicitation have implications for hazard assessment, both for conditional probabilities
500 and the related eruption parameters. Moreover, it is interesting to consider which questions (and related
501 scenarios) are affected by greater uncertainties, both from the point of view of epistemic uncertainty on eruption
502 types conditional probability ("Other eruption" cases) and intra-question uncertainty (i.e. the credible interval
503 distance between the 5th and the 95th percentiles within each question). The two timeframes chosen (i.e. next
504 eruption and next 100 years) enable us also to analyze two different perspectives for the volcanoes. Specifically,
505 in our opinion, the probability density functions of the NE case could be used for preparing a probabilistic hazard
506 map (or to define emergency plans) for immediate use. This could be accomplished either by considering single
507 eruptions, or by combining the different maps obtained for different eruption types, weighted by the appropriate
508 probability of occurrence (Sandri et al. 2016). In this way, it is possible to create a joint probability hazard map,
509 which encompasses effects arising from any of the eruptions considered in this study, according to their relative

510 weights. In contrast, the N100 case allows considering a longer time frame and the possibility on eruptive
511 scenarios that are not mutually exclusive. These probabilities could be used for estimating the total cumulative
512 hazard in the surrounding territory in the next decades.

513
514 The ESPs for which the uncertainty distributions have been quantified include most of those defined by
515 Bonadonna et al. (2012, 2016) as those that need to be parametrized for the majority of existing plume and
516 tephra transport/deposition numerical models. The list defined by Bonadonna et al. (2012, 2016) includes plume
517 height, eruption mass, mass eruption rate (inferred from total mass and eruption duration), total grain-size
518 distribution, and the onset and end of an eruption (defining eruption duration). With the exception of total grain-
519 size distribution (not elicited for the reasons explained in section 3.1), we have therefore provided detailed
520 uncertainty distributions for such ESPs. These distributions are not simply represented by uniform distributions
521 between two extreme values, but they are characterized by a triplet of uncertainty values (5th, 50th, 95th
522 percentiles) and probability density functions obtained by kernel methods. This probabilistic approach is
523 particularly beneficial if such parameterizations are used as inputs to numerical models for generating hazard
524 maps, when iterative re-sampling of the elicited ESP distributions can capture epistemic or aleatoric
525 uncertainties. When possible, the ESPs here defined have been compared with those available from literature. To
526 this purpose, we compiled a list of well-studied eruptions (classified according to prevalent magma composition,
527 VEI, eruptive style, total mass of fallout deposit and plume height) in Table C1 from Appendix C. While this list
528 is limited and reflects the actual availability of detailed data, it however provides a first order comparison to
529 evaluate the robustness of our estimations.

530 In the following two sub-sections, we discuss separately the implications for hazards at Cotopaxi and at
531 Guagua Pichincha volcanoes. Concerning the ESPs for both volcanoes, as pointed out in section 4.1, average
532 plume height has the lowest variability among the alternative scoring methods, likely due to the better
533 availability of plume height measurements of eruptions with similar magnitudes/intensities, both at the studied
534 volcanoes and worldwide (Mastin et al. 2009; Gouhier et al. 2019).

535 5.2.1 Cotopaxi volcano

536 The responses given by the experts were concordant in general and did not show evidence for “school
537 of thoughts” when judging relative probabilities for rhyolitic and andesitic eruptions (i.e. the probability density
538 functions of rhyolitic and andesitic magmas are unimodal for all three scoring methods). However, the high
539 relative probability that an eruption at Cotopaxi will be andesitic is more pronounced for the NE case (Fig. 3a)
540 than for the N100 case (Fig. 3b). The conditional probability of a rhyolitic eruption (as highlighted in section
541 4.1) is substantially lower than that of an andesitic eruption for both the NE and the N100 cases. This reflects the
542 fact that the last rhyolitic eruption dates back to 2.1 ky BP (see section 2.1). Nevertheless it is very uncertain and
543 not negligible, ranging from 0.4% to 50%, with a median probability of 8-12% (mean values 13-20%). We
544 highlight that at Cotopaxi, eruptions involving rhyolitic magmas characterize mostly the early stages of the
545 eruptive history of the volcano and, generally, deposits from old, low-magnitude eruptions are rarely preserved.
546 From this point of view, the conditional probabilities assigned in Table 3, including the “Other type” case, reflect
547 a conservative approach, in which the possibility of the incompleteness of the rhyolitic eruptive record (i.e.
548 under-recording) is taken into consideration. The Plinian and sub-Plinian eruptions involving rhyolitic magmas
549 have therefore a summed mean conditional probability (for the next eruption) of 11-14 %, where the range of
550 different values depends on the method selected. This mean probability is significantly higher for the N100 case
551 (19-23%). In this respect, the mean possibility of having at least one large-magnitude rhyolitic eruption is not
552 negligible, and this has an effect on the expected volcanic hazard, as highlighted with their related ESPs (see
553 below).

554 Considering andesitic eruptions, it is worth commenting on three aspects. First, similarly to rhyolitic
555 eruptions, the possibility of an under-recording of old, low-magnitude andesitic eruptions could also not be
556 excluded, considering that, according to Hall and Mothes (2008), andesitic magmas occurred within the F series
557 (9.6-5.5 ka BP) rhyolitic eruptive episodes (see section 2.1). Second, the summed mean probability of sub-
558 Plinian and Plinian eruptions involving andesitic magmas for the NE case is 19-27%. Besides exhibiting a
559 greater difference between the various scoring methods relative to rhyolitic cases, the conditional probability of a
560 sub-Plinian or Plinian andesitic eruption is significantly higher than that for a rhyolitic eruption of similar size.
561 This is an important point because, as mentioned earlier, the magma type can have an impact on the potential
562 hazards (as implied by the different ranges of ESPs). Third, the “hydrovolcanic/continuous ash emission”
563 eruption type is considered the most probable next eruption, under all scoring methods. This is consistent with
564 Bernard et al. (2016), who underline that, despite the under-representation of VEI 1-2 eruptions in the geologic
565 record, such an eruption type could be the most frequent ones at Cotopaxi (see also Wolf 1904). There is,
566 however, large uncertainty associated with responses on eruption type probabilities, as highlighted by: i) the
567 largest credible intervals between the 5th and 95th percentiles compared to other elicited items, for all three
568 scoring methods and ii) the differences in multi-modal values depending on scoring method (Fig. 3). Moreover,

569 differences between the alternative scoring methods are also greater, a fact that could be largely correlated to the
570 less well-defined features of this eruption type compared to others (e.g. Plinian or sub-Plinian); the implications
571 of this situation, discussed in section 5.1, should be therefore considered. It is important to highlight that, if we
572 consider the sum of the mean probability of occurrences for any sub-Plinian and Plinian type eruption (rhyolitic
573 or andesitic), we obtain a probability, for the next eruption NE, of 30-40%. A comparison of our results with
574 those of Biass and Bonadonna (2013) is not straightforward, due to some differences in the eruption
575 classification scheme. While these authors focus on eruptions with a specific VEI for their analyses, we have
576 used the terminology sub-Plinian and Plinian, which spans between VEIs. Moreover, Biass and Bonadonna
577 (2013) specifically calculated the probabilities of VEI 3, 4, 5 for the next eruption of $VEI \geq 3$ in the next 100
578 years, without considering the occurrence of multiple events of different type in the next 100 years.

579 Nevertheless, we have calculated, from the values in Table 3, the NE and N100 5th, 50th, 95th probability
580 percentiles, and the mean probability of Plinian eruptions involving either rhyolitic or andesitic magmas (CM
581 method only). These values are, respectively, [1.7, 8.7, 31] with mean value 12% for NE, and [2.9, 23, 65] with
582 mean value 27% for N100, and they are both consistent with the sum of the probabilities of VEI 4 and 5
583 eruptions (20.8%) calculated by Biass and Bonadonna (2013) for the next 100 years at Cotopaxi. Specifically, it
584 seems evident that our estimations, which include uncertainty ranges, fully capture the probability calculated by
585 using other datasets.

586 From the point of view of the parameters that are considered (Table 5), rhyolitic Plinian and sub-Plinian
587 eruptions are expected to have longer median durations than their andesitic counterparts; this is consistent
588 between CM, ERF and EW methods. Their uncertainty ranges are, however, slightly more skewed toward 95th
589 percentile values than is the case in the andesitic scenarios. Andesitic eruptions with shorter durations are
590 expected to have average plume height values that are slightly higher than those of rhyolitic eruptions, at least in
591 terms of median values (for CM, ERF and EW). This implies, from a volcanic hazard point of view, a potentially
592 longer duration of eruptive crises and potentially thicker deposits for rhyolitic eruptions than for andesitic ones.
593 The judged longer duration of rhyolitic eruptions with respect to andesitic counterparts is partially confirmed by
594 the eruptions considered in Table C1, since the mean of the durations for rhyolitic and andesitic eruptions are,
595 respectively, 3300 and 790 min (both within our percentile ranges for both sub-Plinian and Plinian of Table 5).
596 Concerning plume height, mean value from Table C1 are, for rhyolitic and andesitic eruptions, 18 and 19 km
597 respectively. We recall, however, that plume height values from Table C1 are maximum plume heights, while
598 our estimates are average plume heights.

599 The judged tephra fallout mass outputs for sub-Plinian and Plinian eruptions (both rhyolitic and
600 andesitic) range from 10^9 to 10^{12} kg, with medians of 10^{10} kg for sub-Plinian and 10^{11} kg for Plinian, comparable
601 to estimations made for similar eruptions at Cotopaxi (Biass and Bonadonna 2011). For
602 hydrovolcanic/continuous ash emission eruptions, the judged tephra fallout mass is lower relative to other
603 eruption types (median values are all around 10^8 kg), but their duration could be fairly long (median > 1 month -
604 see Table 5). Considering the highest conditional probability of these eruptions (both for the NE and the N100),
605 long eruption durations have potentially severe consequences for aviation operations (Bernard et al. 2016) and
606 for crop and greenhouses agriculture, the latter being one of Ecuador's most important sources of income (Knapp
607 2017).

608 5.2.2 *Guagua Pichincha volcano*

609 The case of Guagua Pichincha is less complex than that of Cotopaxi since the composition of erupted
610 magmas and the eruption types are more homogeneous. Nevertheless, the issue of the completeness of the
611 stratigraphic record still remains. Considering the three eruption types on the event tree in Figure 2b, only
612 Vulcanian to dome-forming eruptions (1999-2001 cycle) and Plinian eruptions (AD 1660) have been observed
613 directly. Despite their apparent absence in the geologic record, in our logic tree we have inserted also sub-Plinian
614 eruptions because they are sometimes difficult to distinguish from Plinian eruptions or from large Vulcanian
615 events. No other eruptions with lower VEIs (including phreatic ones) are present in the geological record, a fact
616 that seems to be partially confirmed by the (scarce) historical accounts of the "Historic" cycle (see Table 2).
617 However, similarly to Cotopaxi, the possibility of unrecorded eruptions is not negligible, essentially because
618 Guagua Pichincha is close to a region (to the west) characterized by a wet climate that does not favor
619 preservation of thin volcanic deposits.

620 Consistent with these observations, the probability of "Other type" eruptions has a non-negligible
621 median value of 7.5 - 11 % for the NE case (mean values of 13 - 18%) and 7.9 - 13 % for the N100 case (mean
622 values of 13 - 22%), considering all three scoring methods. The eruption type for which the conditional
623 probability for all the scoring methods and both for the NE and N100 cases is highest is the Vulcanian type
624 (median values are 40 - 55 % and 56-66 % for NE and N100 respectively; mean values of 40 - 51% and 52 -
625 60%), similar to the event that occurred during the 1999-2001 cycle. Again, in this case (as for the
626 "hydrovolcanic/continuous ash emission" case of Cotopaxi, see previous section) greater uncertainties and

627 differences in multimodal values (Fig. 4) arising from the scoring methods are limited and reasonably correlated
628 with the less well-defined features of this eruption type compared to others (e.g. Plinian or sub-Plinian).

629 In this case study, the situation is similar to that of the hydrovolcanic/continuous ash emission eruption
630 for Cotopaxi volcano (see section 5.2.1), where the probability density function of the CM scoring method
631 differs from those of the ERF and EW methods (Table 4 and Fig. 4). We also remark that the summed mean
632 conditional probabilities for Plinian and sub-Plinian eruptions are 26 – 43 % (NE case) and 50 – 58 % (N100
633 case). Pyroclastic density currents are likely to be one of the worst hazards of a Plinian or sub-Plinian eruption at
634 Guagua Pichincha. However, due to topographic constraints, these currents are likely to be confined mainly to
635 the poorly inhabited valleys to the NW and SW of the active crater (Robin et al. 2008). On the other hand, tephra
636 fallout will represent a major hazard for the city of Quito, since there are historical accounts of ash fall during the
637 AD 1660 eruption (Robin et al. 2008) but also during the much smaller AD 1999 Vulcanian eruption (Naumova
638 et al. 2007; Volentik and Houghton 2015).

639 Finally, we underline that: i) ESPs from Table 6 are consistent both with other estimations for Guagua
640 Pichincha volcanoes (e.g. total mass estimated by Barberi et al. 1992 for Layers 3/5) and values reported in
641 Table C1; ii) there is a similarity between the elicited uncertainty distributions of ESPs for Plinian and sub-
642 Plinian eruptions of Guagua Pichincha with those for the same-size eruption types with andesitic magmas at
643 Cotopaxi volcano (Tables 5 and 6). This similarity represents consistent reasoning by our experts, since the
644 magma compositions of Guagua Pichincha products are dacitic to andesitic (Robin et al. 2010).

645 6. Conclusions

646 This paper addresses the probabilities of different explosive eruption types and their main ESPs at
647 Cotopaxi and Guagua Pichincha volcanoes. We analyzed these probabilities from both “next eruption” and “next
648 100 years” perspectives, through the employment of well-established structured expert judgment analysis
649 procedures involving twenty experts with different backgrounds, professional interests and volcanological
650 experiences. Results are presented, for each eruption parameter, as uncertainty distributions based on probability
651 functions defined by three percentiles (5th, 50th and 95th). By employing different scoring methods with different
652 features and advantages (the Classical Model, the Expected Relative Frequency method, and the Equal Weights
653 pooling rule), the user of these elicitation data is given the opportunity to use the results from one single
654 approach or to choose some combination of the results.

655 In addition, Principal Component Analysis was used for sensitivity testing the outcomes from different
656 sub-groups of experts, the latter subdivided in terms of experience (A1/A2 – Experienced researchers/Early-
657 career researchers), background (B1/B2 – Geologists/Mathematicians-Modelers) and institution affiliation at the
658 time of the elicitation (C1/C2 – Clermont-Ferrand/Quito). Analysing results from the Classical Model highlights
659 that the outcomes considering all the experts are equally distant from those of sub-groups C1/C2, while they are
660 closer to those of sub-groups A1 and B1 respectively. In other words, institutional affiliation was not a
661 determinant of overall decision maker (DM) findings, whereas they were somewhat influenced by experienced
662 researchers and by those with geological backgrounds.

663 Further studies should address two aspects: i) the incompleteness of the geologic record for both
664 Cotopaxi and Guagua Pichincha volcanoes; ii) the causes of major sources of uncertainty highlighted by our
665 expert judgment results. With respect to this latter point, an extended discussion of the rationale behind the ESPs
666 estimates and probability forecasts could enhance their scientific impact. This includes the probability of
667 occurrence and the ESPs of small size eruptions (hydrovolcanic/long-lasting ash emission for Cotopaxi,
668 Vulcanian for Guagua Pichincha), the probability of occurrence and the ESPs of the rhyolitic eruptions of
669 Cotopaxi, and the detailing of the ‘other type’ eruptions.

670 Nevertheless, the probability distributions were found to be robust with respect to different density
671 estimation methods and expert aggregation models. Thus, the reported judgments picture the knowledge of the
672 elicited group of experts, and they could only be modulated by any substantial new data set, information or
673 interpretation of the volcanic record of Cotopaxi and Guagua Pichincha volcanoes. Notwithstanding the
674 limitations of the analysis described above, our estimates represent crucial input information for the development
675 of quantitative hazard and risk maps of eruptive phenomena in the region, especially for what concerns the
676 uncertainty quantification. We remark, moreover, that our approach is not inconsistent with previous studies that
677 involved an analysis of the past eruptive record (Biass and Bonadonna 2013). Nevertheless, we present some
678 information that was rather difficult to obtain without using expert judgment techniques. In particular, we
679 performed uncertainty quantification on the probability estimates provided and on the evaluation of the case of
680 more than one type of eruption occurring in the next 100 years.

681
682 With respect to hazard implications for each volcano, the main results are:

- 683 • for Cotopaxi, the most probable next eruption is considered to be a hydrovolcanic/long-lasting
684 ash emission involving andesitic magma, similar to that of AD 2015. However, the chance of a

685 rhyolitic event is not negligible although very uncertain, with a median probability of 8-12%
686 (mean values 13-20%). The median probability that there will be at least one eruption of this
687 type within the next 100 years is 43 - 55% (mean values in 43 - 51%). Despite these eruptions
688 have relatively low magnitude/intensity, their long durations (median of ~1 month) can have a
689 significant negative impact on aviation safety and both crop and greenhouse cultivations. For
690 larger magnitude eruptions (i.e. sub-Plinian and Plinian), rhyolitic ones have lower
691 probabilities of occurrences than andesitic ones, but they could pose a higher threat due to their
692 potential longer durations and larger eruption masses than their andesitic counterparts. As a
693 whole, summing the mean probabilities that the next eruption will be either sub-Plinian or
694 Plinian (whether rhyolitic or andesitic) returns a substantial, significant mean probability of 30
695 - 40%;

- 696 • for Guagua Pichincha, the most probable next eruption is a vulcanian event (similar to that of
697 AD 1999), with a median probability of occurrence of 40 – 55 % (mean values of 40 - 51%).
698 The median probability that within the next 100 years there will be at least one eruption of this
699 type is greater: 55 - 66 % (mean values of 52 - 60%). The larger magnitude eruption types
700 (sub-Plinian or Plinian) have, in turn, a summed mean probability of occurrence for the next
701 eruption of 26 – 43 %, while for the next 100 years the same combined mean probability is of
702 50 – 58 %.

703 In summary, while small or moderate magnitude eruptions are considered most likely candidates for the
704 next eruption at Cotopaxi and at Guagua Pichincha, the elicited event probabilities for violent explosive
705 eruptions represent a plausible prospect at either volcano in the long or short term. Indeed, the possibility exists,
706 at a non-trivial probability, that the next eruption in either case could be on the scale of a sub-Plinian or Plinian
707 eruption.

708 **Appendix A: Performance-based Expert Judgment**

709 In general, with the performance-based elicitation procedure underpinning the Classical Model
710 approach (Cooke 1991; Aspinall 2006), statistical accuracy (e.g. calibration) and informativeness scores are
711 derived for each expert from a set of ‘seed questions’. These items comprise factual questions, the true
712 quantitative values of which an expert is not expected to know precisely but, in respect of which, he/she is
713 expected to provide meaningful credible intervals that capture those values reliably and informatively, by
714 informed reasoning.

715 Concerning the two scores, statistical accuracy (“calibration”) represents the p-value that the expert’s
716 inter-quantile probabilities, summed over several items, match the underlying probability vector sample
717 distribution implied by the 5th, 50th and 95th percentiles, as assessed by the expert per item. If the actual
718 realization values are indeed drawn independently from such a distribution, with quantiles as stated by the
719 expert, then deviations in the expert’s assessments are asymptotically distributed as a chi-square variable with 3
720 degrees of freedom. The corresponding p-value for goodness-of-fit yields a measure of the expert’s statistical
721 accuracy (or calibration). At the same time, the expert’s informativeness score is the degree to which their
722 uncertainty distributions are concentrated; that is, the smaller the distance between the 5th and the 95th
723 percentiles, the more an expert is informative.

724 In general, it can be shown that these two performance-based scores in the Classical Model refer to
725 “orthogonal” properties of the expert’s judgment capability: i.e. their statistical accuracy versus informativeness.
726 The challenge for the expert, therefore, is to optimize their overall performance score – which is the product of
727 these two metrics - by maximizing them jointly. This is a tricky judgmental balancing act: the expert’s
728 performance score will be penalized if they over-accentuate one at the expense of the other by being more
729 precise or more informative in their judgments on a question than their understanding of the uncertainty
730 warrants.

731 With respect to the scoring methods mentioned in Section 3.1, the two performance-based methods CM
732 (the Classical Model: Cooke 1991) and ERF (Expected Relative Frequency method; Flandoli et al. 2011)
733 significantly differ in their scoring metrics: CM evaluates the statistical distribution of the known values with
734 respect to the expert’s percentiles, and, on a second order, the diameter of the corresponding uncertainty range;
735 ERF measures the likelihood of “accurate” judgments, i.e. those relatively close to the true value of a question.

736 Variances of the performance scores, which indicate how they differ, tend to be highest with the CM
737 approach, lower with ERF (and trivially null with the Equal Weights EW rule, which has no performance
738 measure). We remark that for the purpose of defining the global decision makers (DMs) we always performed a
739 weighted combination (probability mixture) of maximum entropy distributions. That is, we did not use triangular
740 functions and quantile pooling when defining the DMs (Bevilacqua, 2016). This differs from the traditional
741 approach followed in the ERF method but simplifies the comparison of the results by focusing only on the
742 differences in the scores. We remark that the calculation of the ERF scores is still based on triangular functions.

743 According to Flandoli et al. (2011), the main outcomes for each scoring methods are:

- 744 • The main advantage of using the CM method is that it is possible to highlight those experts with the
745 best combination of calibration and informativeness scores (these are not measures of each expert's
746 knowledge about the problem but indicate, objectively, their capability to express informative
747 uncertainties about a range of subject matter items). In particular, when group's judgments are pooled,
748 this latter aspect generally produces smaller (and thus more informative) uncertainty bounds between
749 the 5th and 95th percentiles for each question. Moreover, Flandoli et al. (2011) demonstrate that the
750 uncertainty range described by the CM is usually the best estimate of the supposed 'true' uncertainty;
- 751 • In contrast, the EW method describes the maximum uncertainty bounds (pointing toward a more
752 "conservative" approach) but it does not take into account the information about individual expert's
753 calibration (i.e. statistical accuracy) obtained from the seed questionnaire;
- 754 • Finally, the ERF method has been shown by Flandoli et al. (2011) to conceptually provide the most
755 accurate estimates of supposed 'true' central values (i.e. the median values of the distributions).

756 For this study, during the first plenary session, the experts benefited from a detailed presentation of the
757 eruptive history of the two volcanoes considered. Moreover, details about expert judgment techniques have been
758 provided, which has been followed by final discussion on the topics presented. During the first part of the
759 session, the experts were invited to provide their judgments on 16 seed questions. However, two questions had
760 ambiguous formulations, which led to multiple interpretations by the experts. These questions were excluded
761 from the performance scoring analysis for this reason. During the first stage, the experts were also asked to
762 answer two different target questionnaires, respectively for Cotopaxi and Guagua Pichincha, whereby the experts
763 were asked to evaluate the relative conditional probabilities of different eruptive styles/magma compositions
764 over a single specific future timeframe (i.e. the next 100 years). After a first pass through the questions and
765 following discussions with the experts, some issues were identified within the group's responses about several
766 target items for both Cotopaxi and Guagua Pichincha. More specifically, some ambiguities were identified:

- 767 • for the meaning of the term "Magmatic Unrest"
- 768 • for the definition of an "Eruption"
- 769 • in the distinction between "Rhyolitic" and "Andesitic" magmas for Cotopaxi volcano
- 770 • in relation to questions about the future behavior of the volcano, queries were raised about whether the
771 experts were considering "the next eruption" or an eruption in "the next 100 years", despite having separated the
772 two frameworks of NE and N100.

773 In particular, it has been clarified to the participants that in this study the term "eruption" means a period of
774 continuous volcanic activity, where the products erupted have almost the same composition and the geophysical
775 signals are continuous, although fluctuant. In this sense, an eruption is separated from another eruption by a
776 sufficiently long quiescence time (several months to years), where no volcanic activity is observed.

777 Because of these concerns (such issues usually arise with any expert elicitation), some question wordings were
778 changed and other questions added to the set identifying which of the two alternative timeframes should be
779 considered. The experts were then given the opportunity to revise their responses via email after some
780 clarification notes and additional information were circulated to the participants. It is important to underline that
781 experts have not been asked to provide an explanation to their answers.

782 **Appendix B: calculated mean values from probability distributions**

783 In this appendix we report the calculated means for the probability distributions from Tables 3-6. Such
784 values have been calculated for both Cotopaxi (Table B1) and Guagua Pichincha (Table B2). It is worth
785 mentioning that the sum of the mean probabilities of mutually exclusive scenarios sum to 100% in the NE case.
786 In contrast, the sum is greater than 100% in the N100 case, because the possible occurrence of more than one
787 type of eruption in the next 100 years was not excluded.

788

789 **Appendix C: comparison of some ESPs with global data**

790 Table C1 gives the data of the duration of well-studied eruptions involving, respectively, andesitic,
791 dacitic, and rhyolitic magmas. To improve consistency of our approach with the reported data, the definition of
792 eruption used for calculating durations is different with respect to the one reported in Appendix A, and it reflects
793 the definition of eruption duration proposed by Mastin et al. (2009), which is to be the time period over which a
794 significant amount of ash is continuously emitted into the atmosphere. Plume heights are maximum estimations.

795 **References.**

- 796 Andújar J, Martel C, Pichavant M, Samaniego P, Scaillet B, Molina I (2017) Structure of the plumbing system at
797 Tungurahua volcano, Ecuador: insights from phase equilibrium experiments on July–August 2006
798 eruption products. *Journal of Petrology* 58:1249-1278 doi:<https://doi.org/10.1093/petrology/egx054>
- 799 Aspinall WP (2006) Structured elicitation of expert judgment for probabilistic hazard and risk assessment in
800 volcanic eruptions. *Statistics in volcanology* 1:15-30
- 801 Aspinall WP, Carniel R, Jaquet O, Woo G, Hincks T (2006) Using hidden multi-state Markov models with
802 multi-parameter volcanic data to provide empirical evidence for alert level decision-support. *Journal of*
803 *Volcanology and Geothermal Research* 153:112-124
804 doi:<https://doi.org/10.1016/j.jvolgeores.2005.08.010>
- 805 Aspinall WP, Cooke RM (2013) Quantifying scientific uncertainty from expert judgment elicitation. In: Rougier
806 J, Sparks RSJ, Hill LJ (eds) *Risk and uncertainty assessment for natural hazards*. Cambridge University
807 Press, New York, pp 64-99. doi:www.cambridge.org/9781107006195
- 808 Aspinall WP, Woo G (2014) Santorini unrest 2011–2012: an immediate Bayesian belief network analysis of
809 eruption scenario probabilities for urgent decision support under uncertainty. *Journal of Applied*
810 *Volcanology* 3:1-12 doi:<https://doi.org/10.1186/s13617-014-0012-8>
- 811 Aspinall WP, Bevilacqua A, Costa A, Inakura H, Mahony S, Neri A, Sparks RSJ (2019) Probabilistic
812 reconstruction (or forecasting) of distal runouts of large magnitude ignimbrite PDC flows sensitive to
813 topography using mass-dependent inversion models. In: *AGU Fall Meeting 2019, San Francisco, CA,*
814 *USA, 2019*. doi:doi.org/10.1002/essoar.10502300.1
- 815 Barberi F, Ghigliotti M, Macedonio G, Orellana H, Pareschi MT, Rosi M (1992) Volcanic hazard assessment of
816 Guagua Pichincha (Ecuador) based on past behaviour and numerical models. *Journal of Volcanology*
817 *and Geothermal Research* 49:53-68 doi:[https://doi.org/10.1016/0377-0273\(92\)90004-W](https://doi.org/10.1016/0377-0273(92)90004-W)
- 818 Barberi F, Coltelli M, Frullani A, Rosi M, Almeida E (1995) Chronology and dispersal characteristics of recently
819 (last 5000 years) erupted tephra of Cotopaxi (Ecuador): implications for long-term eruptive forecasting.
820 *Journal of Volcanology and Geothermal research* 69:217-239 doi:[https://doi.org/10.1016/0377-](https://doi.org/10.1016/0377-0273(95)00017-8)
821 [0273\(95\)00017-8](https://doi.org/10.1016/0377-0273(95)00017-8)
- 822 Bebbington MS, Cronin SJ (2011) Spatio-temporal hazard estimation in the Auckland Volcanic Field, New
823 Zealand, with a new event-order model. *Bulletin of Volcanology* 73:55-72
824 doi:<https://doi.org/10.1007/s00445-010-0403-6>
- 825 Bebbington MS, Stirling MW, Cronin SJ, Wang T, Jolly G (2018) National-level long-term eruption forecasts by
826 expert elicitation. *Bulletin of Volcanology* 80:56 doi:<https://doi.org/10.1007/s00445-018-1230-4>
- 827 Bernard B, Battaglia J, Proaño A, Hidalgo S, Vásconez F, Hernandez S, Ruiz MC (2016) Relationship between
828 volcanic ash fallouts and seismic tremor: quantitative assessment of the 2015 eruptive period at
829 Cotopaxi volcano, Ecuador. *Bulletin of Volcanology* 78 doi:10.1007/s00445-016-1077-5
- 830 Bevilacqua A, Isaia R, Neri A, Vitale S, Aspinall WP, Bisson M, Flandoli F, Baxter PJ, Bertagnini A, Esposti
831 Ongaro T, Iannuzzi E, Pistolesi M, Rosi M (2015) Quantifying volcanic hazard at Campi Flegrei
832 caldera (Italy) with uncertainty assessment: I. Vent opening maps. *Journal of Geophysical Research:*
833 *Solid Earth* 120:2309-2329 doi:<https://doi.org/10.1002/2014JB011775>
- 834 Bevilacqua A (2016) Doubly stochastic models for volcanic hazard assessment at Campi Flegrei caldera. PhD
835 Theses. Birkhäuser/Springer, Pisa. doi:<https://doi.org/10.1007/978-88-7642-577-6>
- 836 Bevilacqua A, Flandoli F, Neri A, Isaia R, Vitale S (2016) Temporal models for the episodic volcanism of
837 Campi Flegrei caldera (Italy) with uncertainty quantification. *Journal of Geophysical Research: Solid*
838 *Earth* 121:7821-7845 doi:<https://doi.org/10.1002/2016JB013171>
- 839 Bevilacqua A, Bursik MI, Patra AK, Pitman BE, Yang Q, Sangani R, Kobs- Nawotniak S (2018) Late
840 Quaternary eruption record and probability of future volcanic eruptions in the Long Valley volcanic
841 region (CA, USA). *Journal of Geophysical Research: Solid Earth* 123:5466-5494
842 doi:<https://doi.org/10.1029/2018JB015644>
- 843 Bevilacqua A, Pitman EB, Patra AK, Neri A, Bursik MI, Voight B (2019) Probabilistic enhancement of the
844 Failure Forecast Method using a stochastic differential equation and application to volcanic eruption
845 forecasts. *Frontiers in Earth Science* 7 doi:<https://doi.org/10.3389/feart.2019.00135>
- 846 Bevilacqua A, Bertagnini A, Pompilio M, Landi P, Del Carlo P, Di Roberto A, Aspinall WP, Neri A (2020a)
847 Major explosions and paroxysms at Stromboli (Italy): a new historical catalog and temporal models of
848 occurrence with uncertainty quantification. *Scientific Reports* 10 doi:[https://doi.org/10.1038/s41598-](https://doi.org/10.1038/s41598-020-74301-8)
849 [020-74301-8](https://doi.org/10.1038/s41598-020-74301-8)
- 850 Bevilacqua A, Patra AK, Pitman EB, Bursik MI, De Martino P, Giudicepietro F, Macedonio G, Vitale S,
851 Flandoli F, Voight B (2020b) Utilizzo preliminare del failure forecast method sui dati GPS di
852 spostamento orizzontale registrati nella caldera dei Campi Flegrei dal 2011 al 2020. *Miscellanea INGV*
853 57:135-139 doi:<https://doi.org/10.13127/misc/57/25> English version: arXiv:2007.02756

854 Bevilacqua A, Patra AK, Pitman EB, Bursik MI, De Martino P, Giudicepietro F, Ricciolino P, Macedonio G,
855 Vitale S, Flandoli F, Voight B (2020c) The Failure Forecast Method applied to the GPS and seismic
856 data collected in the Campi Flegrei caldera (Italy) in 2011-2020. In: AGU Fall Meeting, San Francisco,
857 1-17/12/2020 2020c. doi:<https://doi.org/10.1002/essoar.10505832.1>

858 Biass S, Bonadonna C (2011) A quantitative uncertainty assessment of eruptive parameters derived from tephra
859 deposits: the example of two large eruptions of Cotopaxi volcano, Ecuador. *Bulletin of Volcanology*
860 73:73-90

861 Biass S, Bonadonna C (2013) A fast GIS-based risk assessment for tephra fallout: the example of Cotopaxi
862 volcano, Ecuador. *Natural Hazards* 65:477-495 doi:<https://doi.org/10.1007/s11069-012-0378-z>

863 Biass S, Frischknecht C, Bonadonna C (2013) A fast GIS-based risk assessment for tephra fallout: the example
864 of Cotopaxi volcano, Ecuador - Part II: vulnerability and risk assessment. *Natural hazards* 65:497-521
865 doi:<https://doi.org/10.1007/s11069-012-0457-1>

866 Biass S, Scaini C, Bonadonna C, Folch A, Smith K, Höskuldsson A (2014) A multi-scale risk assessment for
867 tephra fallout and airborne concentration from multiple Icelandic volcanoes-Part 1: Hazard assessment.
868 *Natural Hazards and Earth System Sciences* 14:2265 doi:10.5194/nhess-14-2265-2014

869 Biass S, Todde A, Cioni R, Pistolesi M, Geshi N, Bonadonna C (2017) Potential impacts of tephra fallout from a
870 large-scale explosive eruption at Sakurajima volcano, Japan. *Bulletin of Volcanology* 79:73
871 doi:<https://doi.org/10.1007/s00445-017-1153-5>

872 Bonadonna C, Phillips JC (2003) Sedimentation from strong volcanic plumes. *Journal of Geophysical Research:*
873 *Solid Earth* 108 doi:<https://doi.org/10.1029/2002JB002034>

874 Bonadonna C, Connor CB, Houghton BF, Connor LJ, Byrne M, Laing A, Hincks TK (2005) Probabilistic
875 modeling of tephra dispersal: Hazard assessment of a multiphase rhyolitic eruption at Tarawera, New
876 Zealand. *Journal of Geophysical Research: Solid Earth* 110 doi:<https://doi.org/10.1029/2003JB00289>

877 Bonadonna C, Folch A, Loughlin S, Puempel H (2012) Future developments in modelling and monitoring of
878 volcanic ash clouds: outcomes from the first IAVCEI-WMO workshop on Ash Dispersal Forecast and
879 Civil Aviation. *Bulletin of volcanology* 74:1-10 doi:<https://doi.org/10.1007/s00445-011-0508-6>

880 Bonadonna C, Cioni R, Pistolesi M, Elissondo M, Baumann V (2015) Sedimentation of long-lasting wind-
881 affected volcanic plumes: the example of the 2011 rhyolitic Cordón Caulle eruption, Chile. *Bulletin of*
882 *Volcanology* 77:13

883 Bonadonna C, Cioni R, Costa A, Druitt TH, Phillips JC, Pioli L, Andronico D, Harris AJL, Scollo S, Bachmann
884 O, Bagheri G, Biass S, Brogi F, Cashman KV, Dominguez L, Dürig T, Galland O, Giordano G,
885 Gudmundsson M, Hort M, Höskuldsson Á, Houghton BF, Komorowski JC, Küppers U, Lacanna G, Le
886 Pennec JL, Macedonio G, Manga M, Manzella I, de'Michieli Vitturi M, Neri A, Pistolesi M, Polacci M,
887 Ripepe M, Rossi E, Scheu B, Sulpizio R, Tripoli B, Valade S, Valentine GA, Vidal C, Wallenstein N
888 (2016) MeMoVolc report on classification and dynamics of volcanic explosive eruptions. *Bulletin of*
889 *volcanology* 78:84 doi:<https://doi.org/10.1007/s00445-016-1071-y>

890 Bonasia R, Capra L, Costa A, Macedonio G, Saucedo R (2011) Tephra fallout hazard assessment for a Plinian
891 eruption scenario at Volcán de Colima (Mexico). *Journal of Volcanology and Geothermal Research*
892 203:12-22 doi:<https://doi.org/10.1016/j.jvolgeores.2011.03.006>

893 Carey RJ, Houghton BF, Thordarson T (2010) Tephra dispersal and eruption dynamics of wet and dry phases of
894 the 1875 eruption of Askja Volcano, Iceland. *Bulletin of Volcanology* 72:259-278
895 doi:<https://doi.org/10.1007/s00445-009-0317-3>

896 Chiasera B, Cortés JA (2011) Predictive regions for geochemical compositional data of volcanic systems.
897 *Journal of Volcanology and Geothermal Research* 207:83-92
898 doi:<https://doi.org/10.1016/j.jvolgeores.2011.07.009>

899 Christophersen A, Deligne NI, Hanea AM, Chardot L, Fournier N, Aspinall WP (2018) Bayesian Network
900 modeling and expert elicitation for probabilistic eruption forecasting: pilot study for Whakaari/White
901 Island, New Zealand. *Frontiers in Earth Science* 6:211 doi:<https://doi.org/10.3389/feart.2018.00211>

902 Coles SG, Sparks RSJ (2006) Extreme value methods for modelling historical series of large volcanic
903 magnitudes. In: Mader HM, Coles SG, Connor CB, Connor LJ (eds) *Statistics in volcanology*, vol 1.
904 IAVCEI Speial Publication. Geological Society, London, pp 47-56

905 Connor CB, Connor LJ (2009) *Estimating spatial density with kernel methods. Volcanic and tectonic hazard*
906 *assessment for nuclear facilities* Cambridge University Press, Cambridge, UK:346-368

907 Connor CB, Bebbington MS, Marzocchi W (2015) Probabilistic volcanic hazard assessment. In: Sigurdsson H,
908 Houghton BF, McNutt SR, Rymer H, Stix J (eds) *The Encyclopedia of Volcanoes*. Elsevier, pp 897-
909 910. doi:<https://doi.org/10.1016/B978-0-12-385938-9.00051-1>

910 Cooke RM (1991) Experts in uncertainty: opinion and subjective probability in science.

911 Costa A, Dell'Erba F, Di Vito MA, Isaia R, Macedonio G, Orsi G, Pfeiffer T (2009) Tephra fallout hazard
912 assessment at the Campi Flegrei caldera (Italy). *Bulletin of Volcanology* 71:259
913 doi:<https://doi.org/10.1007/s00445-008-0220-3>

914 Costa A, Pioli L, Bonadonna C (2016) Assessing tephra total grain-size distribution: Insights from field data
915 analysis. *Earth and Planetary Science Letters* 443:90-107 doi:<https://doi.org/10.1016/j.epsl.2016.02.040>

916 De la Cruz-Reyna S (1993) Random patterns of occurrence of explosive eruptions at Colima Volcano, Mexico.
917 *Journal of Volcanology and Geothermal research* 55:51-68 doi:[https://doi.org/10.1016/0377-0273\(93\)90089-A](https://doi.org/10.1016/0377-0273(93)90089-A)

918

919 Deligne NI, Coles SG, Sparks RSJ (2010) Recurrence rates of large explosive volcanic eruptions. *Journal of*
920 *Geophysical Research: Solid Earth* 115 doi:<https://doi.org/10.1029/2009JB006554>

921 Deligne NI, Sparks RSJ, Brown SK (2017) Report on potential sampling biases in the LaMEVE database of
922 global volcanism. *Journal of Applied Volcanology* 6:1-5 doi:<https://doi.org/10.1186/s13617-017-0058-5>

923

924 Durant AJ, Villarosa G, Rose WI, Delmelle P, Prata AJ, Viramonte JG (2012) Long-range volcanic ash transport
925 and fallout during the 2008 eruption of Chaitén volcano, Chile. *Physics and Chemistry of the Earth,*
926 *Parts A/B/C* 45:50-64 doi:<https://doi.org/10.1016/j.pce.2011.09.004>

927 Flandoli F, Giorgi E, Aspinall WP, Neri A (2011) Comparison of a new expert elicitation model with the
928 Classical Model, equal weights and single experts, using a cross-validation technique. *Reliability*
929 *Engineering & System Safety* 96:1292-1310 doi:<https://doi.org/10.1016/j.res.2011.05.012>

930 Furlan C (2010) Extreme value methods for modelling historical series of large volcanic magnitudes. *Statistical*
931 *Modelling* 10:113-132 doi:<https://doi.org/10.1177/1471082X0801000201>

932 Garcia-Aristizabal A, Kumagai H, Samaniego P, Mothes P, Yepes H, Monzier M (2007) Seismic, petrologic,
933 and geodetic analyses of the 1999 dome-forming eruption of Guagua Pichincha volcano, Ecuador.
934 *Journal of volcanology and geothermal research* 161:333-351
935 doi:<https://doi.org/10.1016/j.jvolgeores.2006.12.007>

936 Gaunt HE, Bernard B, Hidalgo S, Proaño A, Wright HM, Mothes P, Criollo E, Kueppers U (2016) Juvenile
937 magma recognition and eruptive dynamics inferred from the analysis of ash time series: The 2015
938 reawakening of Cotopaxi volcano. *Journal of Volcanology and Geothermal Research* 328:134-146
939 doi:<https://doi.org/10.1016/j.jvolgeores.2016.10.013>

940 Geotermica Italiana (1989) Mitigación del Riesgo Volcanico en el Area Metropolitana de Quito. Ministerio
941 Affari Esteri Italiano, Pisa

942 Global Volcanism Program (2013) *Volcanoes of the world*, v. 4.8.7, E. Venzke, Smithsonian Institution.
943 Accessed 18/03/2020

944 Gouhier M, Eychenne J, Azzaoui N, Guillin A, Deslandes M, Poret M, Costa A, Husson P (2019) Low
945 efficiency of large volcanic eruptions in transporting very fine ash into the atmosphere. *Scientific*
946 *reports* 9:1-12 doi:<https://doi.org/10.1038/s41598-019-38595-7>

947 Hall ML, Mothes PA (2008) The rhyolitic–andesitic eruptive history of Cotopaxi volcano, Ecuador. *Bull Volc*
948 *70:675-702* doi:<https://doi.org/10.1007/s00445-007-0161-2>

949 Hidalgo S, Battaglia J, Arellano S, Sierra D, Bernard B, Parra R, Kelly P, Dinger F, Barrington C, Samaniego P
950 (2018) Evolution of the 2015 Cotopaxi eruption revealed by combined geochemical and seismic
951 observations. *Geochemistry, Geophysics, Geosystems* 19:2087-2108
952 doi:<https://doi.org/10.1029/2018GC007514>

953 Hincks TK, Komorowski JC, Sparks RSJ, Aspinall WP (2014) Retrospective analysis of uncertain eruption
954 precursors at La Soufrière volcano, Guadeloupe, 1975–77: volcanic hazard assessment using a Bayesian
955 Belief Network approach. *Journal of Applied Volcanology* 3:3 doi:<https://doi.org/10.1186/2191-5040-3-3>

956

957 Kilburn CRJ (2018) Forecasting volcanic eruptions: beyond the Failure Forecast Method. *Frontiers in Earth*
958 *Science* 6:133 doi:<https://doi.org/10.3389/feart.2018.00133>

959 Kiyosugi K, Connor CB, Sparks RSJ, Crowweller HS, Brown SK, Siebert L, Wang T, Takarada S (2015) How
960 many explosive eruptions are missing from the geologic record? Analysis of the quaternary record of
961 large magnitude explosive eruptions in Japan. *Journal of Applied Volcanology* 4:1-15
962 doi:<https://doi.org/10.1186/s13617-015-0035-9>

963 Knapp G (2017) Mountain agriculture for global markets: The case of greenhouse floriculture in Ecuador.
964 *Annals of the American Association of Geographers* 107:511-519
965 doi:<https://doi.org/10.1080/24694452.2016.1203282>

966 Macedonio G, Costa A, Scollo S, Neri A (2016) Effects of eruption source parameter variation and
967 meteorological dataset on tephra fallout hazard assessment: example from Vesuvius (Italy). *Journal of*
968 *Applied Volcanology* 5:1

969 Martel C, Andújar J, Mothes P, Scaillet B, Pichavant M, Molina I (2018) Storage conditions of the mafic and
970 silicic magmas at Cotopaxi, Ecuador. *Journal of Volcanology and Geothermal Research* 354:74-86

971 Martí J, Aspinall WP, Sobradelo R, Felpeto A, Geyer A, Ortiz R, Baxter PJ, Cole PD, Pacheco J, Blanco MJ
972 (2008) A long-term volcanic hazard event tree for Teide-Pico Viejo stratovolcanoes (Tenerife, Canary

973 Islands). *Journal of Volcanology and Geothermal Research* 178:543-552
974 doi:<https://doi.org/10.1016/j.jvolgeores.2008.09.023>

975 Marzocchi W, Bebbington MS (2012) Probabilistic eruption forecasting at short and long time scales. *Bulletin of*
976 *volcanology* 74:1777-1805 doi:<https://doi.org/10.1007/s00445-012-0633-x>

977 Mastin LG, Guffanti M, Servranckx R, Webley P, Barsotti S, Dean K, Durant AJ, Ewert JW, Neri A, Rose WI,
978 Schneider D, Siebert L, Stunder BJB, Swanson G, Tupper A, Volentik ACM, Waythomas CF (2009) A
979 multidisciplinary effort to assign realistic source parameters to models of volcanic ash-cloud transport
980 and dispersion during eruptions. *Journal of Volcanology and Geothermal Research* 186:10-21
981 doi:<https://doi.org/10.1016/j.jvolgeores.2009.01.008>

982 Mothes PA, Hall ML, Janda RJ (1998) The enormous Chillos Valley Lahar: an ash-flow-generated debris flow
983 from Cotopaxi Volcano, Ecuador. *Bulletin of Volcanology* 59:233-244
984 doi:<https://doi.org/10.1007/s004450050188>

985 Mulargia F, Tinti S, Boschi E (1985) A statistical analysis of flank eruptions on Etna volcano. *Journal of*
986 *volcanology and geothermal research* 23:263-272 doi:[https://doi.org/10.1016/0377-0273\(85\)90037-X](https://doi.org/10.1016/0377-0273(85)90037-X)

987 Naumova EN, Yepes H, Griffiths JK, Sempértegui F, Khurana G, Jagai JS, Játiva E, Estrella B (2007)
988 Emergency room visits for respiratory conditions in children increased after Guagua Pichincha volcanic
989 eruptions in April 2000 in Quito, Ecuador observational study: time series analysis. *Environmental*
990 *Health* 6:21 doi:<https://doi.org/10.1186/1476-069X-6-21>

991 Neri A, Aspinall WP, Cioni R, Bertagnini A, Baxter PJ, Zuccaro G, Andronico D, Barsotti S, Cole PD, Esposti
992 Ongaro T (2008) Developing an event tree for probabilistic hazard and risk assessment at Vesuvius.
993 *Journal of Volcanology and Geothermal Research* 178:397-415
994 doi:<https://doi.org/10.1016/j.jvolgeores.2008.05.014>

995 Newhall CG, Hoblitt RP (2002) Constructing event trees for volcanic crises. *Bulletin of Volcanology* 64:3-20
996 doi:<https://doi.org/10.1007/s004450100173>

997 Papale P (2018) Global time-size distribution of volcanic eruptions on Earth. *Scientific reports* 8:1-11
998 doi:<https://doi.org/10.1038/s41598-018-25286-y>

999 Parra R, Bernard B, Narváez D, Le Pennec JL, Hasselle N, Folch A (2016) Eruption Source Parameters for
1000 forecasting ash dispersion and deposition from vulcanian eruptions at Tungurahua volcano: Insights
1001 from field data from the July 2013 eruption. *Journal of Volcanology and Geothermal Research* 309:1-13
1002 doi:<https://doi.org/10.1016/j.jvolgeores.2015.11.001>

1003 Pistolesi M, Rosi M, Cioni R, Cashman KV, Rossotti A, Aguilera E (2011) Physical volcanology of the post-
1004 twelfth-century activity at Cotopaxi volcano, Ecuador: Behavior of an andesitic central volcano.
1005 *Geological Society of America Bulletin* 123:1193-1215 doi:<https://doi.org/10.1130/B30301.1>

1006 Poland MP, Anderson KR (2020) Partly Cloudy With a Chance of Lava Flows: Forecasting Volcanic Eruptions
1007 in the Twenty- First Century. *Journal of Geophysical Research: Solid Earth* 125
1008 doi:<https://doi.org/10.1029/2018JB016974>

1009 Riley CM, Rose WI, Bluth GJS (2003) Quantitative shape measurements of distal volcanic ash. *Journal of*
1010 *Geophysical Research: Solid Earth* 108 doi:<https://doi.org/10.1029/2001JB000818>

1011 Risacher F, Alonso H (2001) Geochemistry of ash leachates from the 1993 Lascar eruption, northern Chile.
1012 Implication for recycling of ancient evaporites. *Journal of volcanology and geothermal research*
1013 109:319-337 doi:[https://doi.org/10.1016/S0377-0273\(01\)00198-6](https://doi.org/10.1016/S0377-0273(01)00198-6)

1014 Robertson RM, Kilburn CRJ (2016) Deformation regime and long-term precursors to eruption at large calderas:
1015 Rabaul, Papua New Guinea. *Earth and Planetary Science Letters* 438:86-94
1016 doi:<https://doi.org/10.1016/j.epsl.2016.01.003>

1017 Robin C, Samaniego P, Le Pennec JL, Mothes PM, Van Der Plicht J (2008) Late Holocene phases of dome
1018 growth and Plinian activity at Guagua Pichincha volcano (Ecuador). *J Volcanol Geoth Res* 176:7-15
1019 doi:<https://doi.org/10.1016/j.jvolgeores.2007.10.008>

1020 Robin C, Samaniego P, Le Pennec JL, Fornari M, Mothes PA, Van Der Plicht J (2010) New radiometric and
1021 petrological constraints on the evolution of the Pichincha volcanic complex (Ecuador). *Bulletin of*
1022 *volcanology* 72:1109-1129 doi:<https://doi.org/10.1007/s00445-010-0389-0>

1023 Rougier J, Sparks RSJ, Cashman KV (2016) Global recording rates for large eruptions. *Journal of Applied*
1024 *Volcanology* 5:1-10 doi:<https://doi.org/10.1186/s13617-016-0051-4>

1025 Rougier J, Sparks RSJ, Cashman KV (2018) Regional and global under-recording of large explosive eruptions in
1026 the last 1000 years. *Journal of Applied Volcanology* 7:1-10 doi:<https://doi.org/10.1186/s13617-017-0070-9>

1027

1028 Runge MG, Bebbington MS, Cronin SJ, Lindsay JM, Kenedi CL, Moufti MRH (2014) Vents to events:
1029 determining an eruption event record from volcanic vent structures for the Harrat Rahat, Saudi Arabia.
1030 *Bulletin of Volcanology* 76:804 doi:<https://doi.org/10.1007/s00445-014-0804-z>

1031 Samaniego P, Robin C, Chazot G, Bourdon E, Cotten J (2010) Evolving metasomatic agent in the Northern
1032 Andean subduction zone, deduced from magma composition of the long-lived Pichincha volcanic

1033 complex (Ecuador). *Contributions to Mineralogy and Petrology* 160:239-260
1034 doi:<https://doi.org/10.1007/s00410-009-0475-5>

1035 Sandri L, Costa A, Selva J, Tonini R, Macedonio G, Folch A, Sulpizio R (2016) Beyond eruptive scenarios:
1036 assessing tephra fallout hazard from Neapolitan volcanoes. *Scientific reports* 6:1-13
1037 doi:<https://doi.org/10.1038/srep24271>

1038 Sheldrake TE (2014) Long-term forecasting of eruption hazards: A hierarchical approach to merge analogous
1039 eruptive histories. *Journal of volcanology and geothermal research* 286:15-23
1040 doi:<https://doi.org/10.1016/j.jvolgeores.2014.08.021>

1041 Sheldrake TE, Sparks RSJ, Cashman KV, Wadge G, Aspinall WP (2016) Similarities and differences in the
1042 historical records of lava dome-building volcanoes: Implications for understanding magmatic processes
1043 and eruption forecasting. *Earth-Science Reviews* 160:240-263
1044 doi:<https://doi.org/10.1016/j.earscirev.2016.07.013>

1045 Silverman BW (1986) *Density estimation for statistics and data analysis*. vol 26. CRC press,

1046 Smyth MA, Clapperton C (1986) Late Quaternary volcanic debris avalanche at Cotopaxi, Ecuador. *Revista*
1047 *Centro Interandino Americano de Fotointerpretación CIAF (Bogotá)* 11:24-38

1048 Tadini A, Bevilacqua A, Neri A, Cioni R, Aspinall WP, Bisson M, Isaia R, Mazzarini F, Valentine GAV, Vitale
1049 S, Baxter PJ, Bertagnini A, Cerminara M, de' Michieli Vitturi M, Di Roberto A, Engwell SL, Esposti
1050 Ongaro T, Flandoli F, Pistolesi M (2017a) Assessing future vent opening locations at the Somma-
1051 Vesuvio volcanic complex: 2. Probability maps of the caldera for a future Plinian/sub-Plinian event
1052 with uncertainty quantification. *Journal of Geophysical Research: Solid Earth* 122:4357-4376
1053 doi:10.1002/2016JB013860

1054 Tadini A, Bisson M, Neri A, Cioni R, Bevilacqua A, Aspinall WP (2017b) Assessing future vent opening
1055 locations at the Somma-Vesuvio volcanic complex: 1. A new information geo-database with uncertainty
1056 characterizations. *Journal of Geophysical Research: Solid Earth* 122:4336-4356
1057 doi:10.1002/2016JB013858

1058 Tadini A, Roche O, Samaniego P, Guillin A, Azzaoui N, Gouhier M, de' Michieli Vitturi M, Pardini F, Eychenne
1059 J, Bernard B (2020) Quantifying the uncertainty of a coupled plume and tephra dispersal model:
1060 PLUME- MOM/HYSPLIT simulations applied to Andean volcanoes. *Journal of Geophysical Research:*
1061 *Solid Earth* 125 doi:<https://doi.org/10.1029/2019JB018390>

1062 Tierz P, Clarke B, Calder ES, Dessalegn F, Lewi E, Yirgu G, Fontijn K, Crummy JM, Bekele Y, Loughlin SC
1063 (2020) Event trees and epistemic uncertainty in long-term volcanic hazard assessment of rift
1064 volcanoes: the example of Aluto (Central Ethiopia). *Geochemistry, Geophysics, Geosystems*
1065 doi:<https://doi.org/10.1029/2020GC009219>

1066 Tsunematsu K, Bonadonna C (2015) Grain-size features of two large eruptions from Cotopaxi volcano (Ecuador)
1067 and implications for the calculation of the total grain-size distribution. *Bulletin of Volcanology* 77:64
1068 doi:<https://doi.org/10.1007/s00445-015-0949-4>

1069 Vázquez R, Bonasia R, Folch A, Arce JL, Macías JL (2019) Tephra fallout hazard assessment at Tacaná volcano
1070 (Mexico). *Journal of South American Earth Sciences* 91:253-259
1071 doi:<https://doi.org/10.1016/j.jsames.2019.02.013>

1072 Vezzoli L, Apuani T, Corazzato C, Uttini A (2017) Geological and geotechnical characterization of the debris
1073 avalanche and pyroclastic deposits of Cotopaxi Volcano (Ecuador). A contribute to instability-related
1074 hazard studies. *Journal of Volcanology and Geothermal Research* 332:51-70
1075 doi:<https://doi.org/10.1016/j.jvolgeores.2017.01.004>

1076 Voight B (1988) A method for prediction of volcanic eruptions. *Nature* 332:125-130
1077 doi:<https://doi.org/10.1038/332125a0>

1078 Volentik ACM, Houghton BF (2015) Tephra fallout hazards at Quito International Airport (Ecuador). *Bulletin of*
1079 *Volcanology* 77:50 doi:<https://doi.org/10.1007/s00445-015-0923-1>

1080 Wang T, Bebbington MS (2012) Estimating the likelihood of an eruption from a volcano with missing onsets in
1081 its record. *Journal of volcanology and geothermal research* 243:14-23
1082 doi:<https://doi.org/10.1016/j.jvolgeores.2012.06.032>

1083 Wold S, Esbensen K, Geladi P (1987) Principal component analysis. *Chemometrics and intelligent laboratory*
1084 *systems* 2:37-52 doi:[https://doi.org/10.1016/0169-7439\(87\)80084-9](https://doi.org/10.1016/0169-7439(87)80084-9)

1085 Wolf T (1904) *Crónica de los fenómenos volcánicos y terremotos en el Ecuador con algunas noticias sobre otros*
1086 *países de la América Central y Meridional desde 1535 hasta 1797*. Imprenta de la Universidad Central
1087 de Quito, Quito. doi:<http://www.dspace.uce.edu.ec/handle/25000/14200>

1088 Wright HMN, Cashman KV, Rosi M, Cioni R (2007) Breadcrust bombs as indicators of Vulcanian eruption
1089 dynamics at Guagua Pichincha volcano, Ecuador. *Bulletin of Volcanology* 69:281-300
1090 doi:<https://doi.org/10.1007/s00445-006-0073-6>

1091
1092

1093
1094
1095
1096
1097
1098
1099
1100
1101
1102
1103
1104
1105
1106
1107
1108
1109
1110
1111
1112
1113
1114
1115
1116
1117
1118
1119
1120
1121
1122
1123
1124
1125
1126
1127
1128
1129
1130
1131
1132
1133
1134
1135
1136
1137
1138
1139
1140
1141
1142
1143
1144
1145
1146
1147
1148
1149
1150
1151

FIGURE CAPTIONS

Figure 1. a) Location of Cotopaxi and Guagua Pichincha volcanoes. b) and c) are enlargements of a). Coordinates expressed in the UTM WGS84 17S coordinate system. Service Layer Credits, source: Esri, DigitalGlobe, GeoEye, Earthstar Geographics, CNES/Airbus DS, USDA, USGS, AeroGRID, IGN and the GIS User Community.

Figure 2. Logic trees for a) Cotopaxi and b) Guagua Pichincha volcanoes. Each of the lowest branch of the logic trees represents a possible eruptive scenario with the maximum expected eruptive style.

Figure 3. Cotopaxi volcano. Probability density functions of conditional probabilities for a) the next eruption and b) the next 100 years. For each graph, it is reported on the x-axis the Decision Maker's response (in %), and on the y-axis the distributions of, respectively, the Classical Model (red), the Expected Relative Frequency (blue) and the Equal Weight (green) Decision Makers.

Figure 4. Guagua Pichincha volcano. Probability density functions of conditional probabilities for a) the next eruption and b) the next 100 years. For each graph, it is reported on the x-axis the Decision Maker's response (in %), and the distributions of, respectively, the Classical Model (red), the Expected Relative Frequency (blue) and the Equal Weight (green) Decision Makers.

Figure 5. Eigenvectors of the different sub-groups (A1 – Senior researchers; A2 – Early-career researchers; B1 – Geologists; B2 – Mathematicians/Modelers; C1 – Clermont-Ferrand; C2 – Quito) plotted against the eigenvector of the whole group of experts (All). All the eigenvectors have been derived from the solutions of the Classical Model (CM) listed in Tables 3-6. Dim1 and Dim2 are the percentages of the x and y component of each eigenvector.

TABLE CAPTIONS

Table 1. Selected eruptions from Cotopaxi volcano used to define the typologies of eruption that compose logic trees of Figure 2. References: ¹Hall and Mothes (2008); ²Pistolesi et al. (2011); ³Tsunematsu and Bonadonna (2015); ⁴Bernard et al. (2016).

Table 2. Selected eruptions from Guagua Pichincha volcano used to define the typologies of eruption that compose logic trees of Figure 2. References: ¹Barberi et al. (1992); ²Robin et al. (2008); ³Robin et al. (2010).

Table 3. Conditional probabilities of different eruption types for the “next eruption” (NE) and “next 100 years” (N100) cases at Cotopaxi.

Table 4. Conditional probabilities of different eruption types for the “next eruption” (NE) and “next 100 years” (N100) cases at Guagua Pichincha.

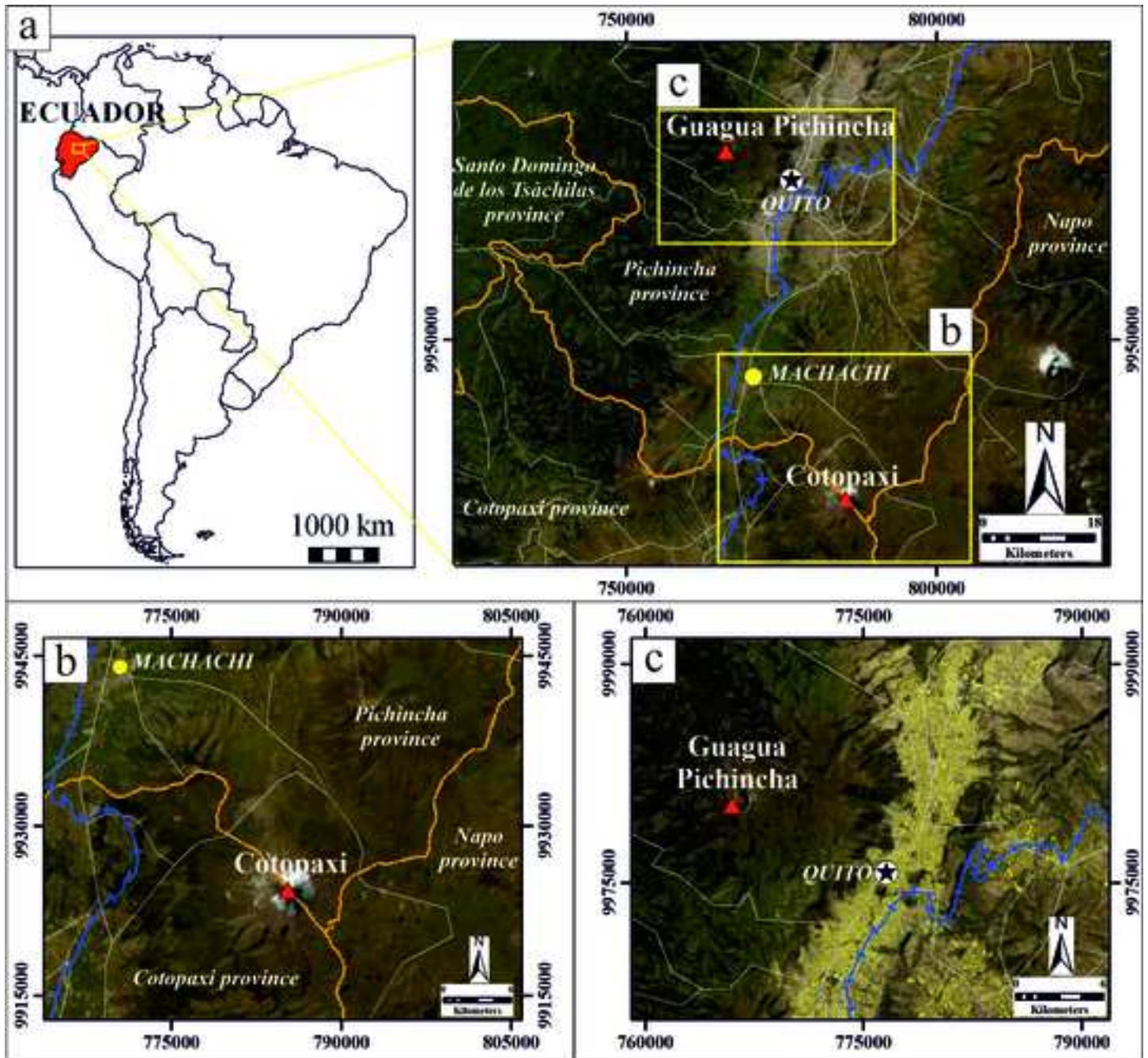
Table 5. Uncertainty ranges for eruptive source parameters of Cotopaxi volcano. For durations, 1 day = 1440 min., 1 week = 10080 min., 1 month = 43200 min., 1 year = 525600 min.

Table 6. Uncertainty ranges for eruptive source parameters of Guagua Pichincha volcano. For durations, 1 day = 1440 min., 1 week = 10080 min., 1 month = 43200 min., 1 year = 525600 min.

Table B1. Mean values for the probability of occurrences (next eruption NE and next 100 years N100) for the classical model (CM), expected relative frequency (ERF) and equal weight (EW) rule for Cotopaxi and Guagua Pichincha volcanoes.

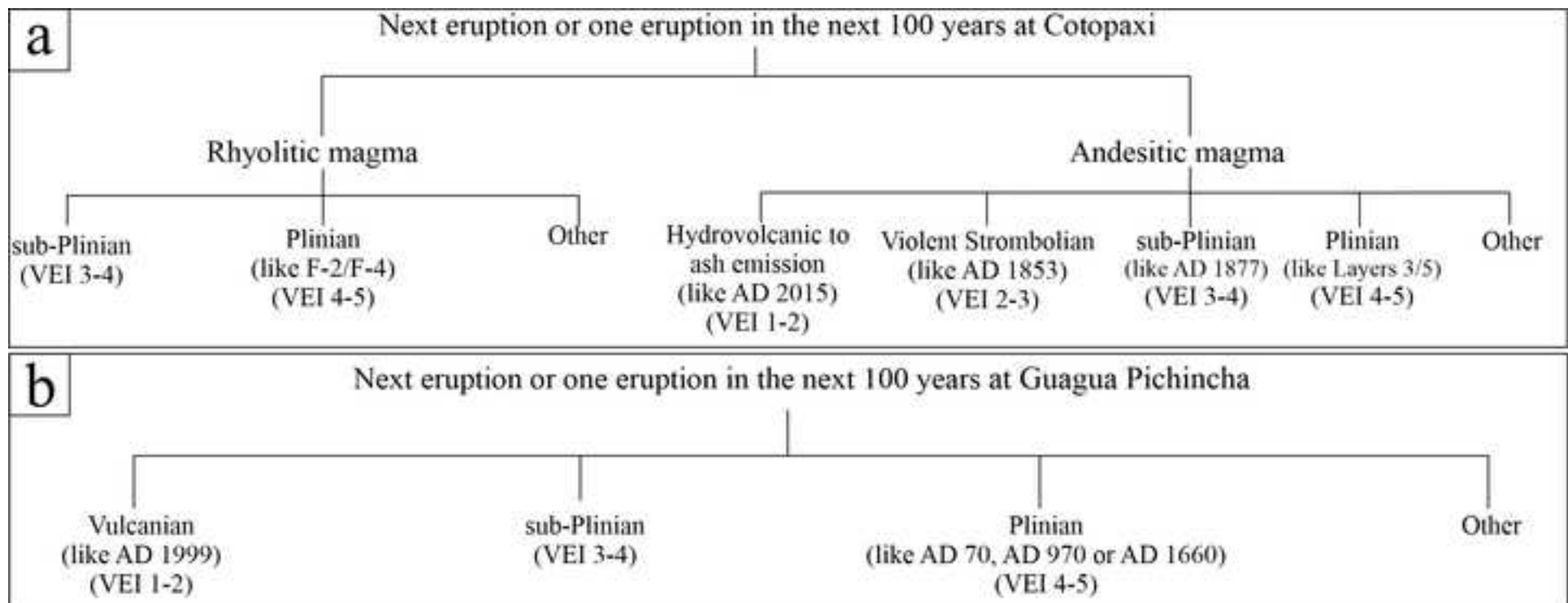
Table B2. Mean values for the eruptive source parameters (duration, total mass of the tephra fallout deposit and average plume height) for the classical model (CM), expected relative frequency (ERF) and equal weight (EW) rule for Cotopaxi and Guagua Pichincha volcanoes.

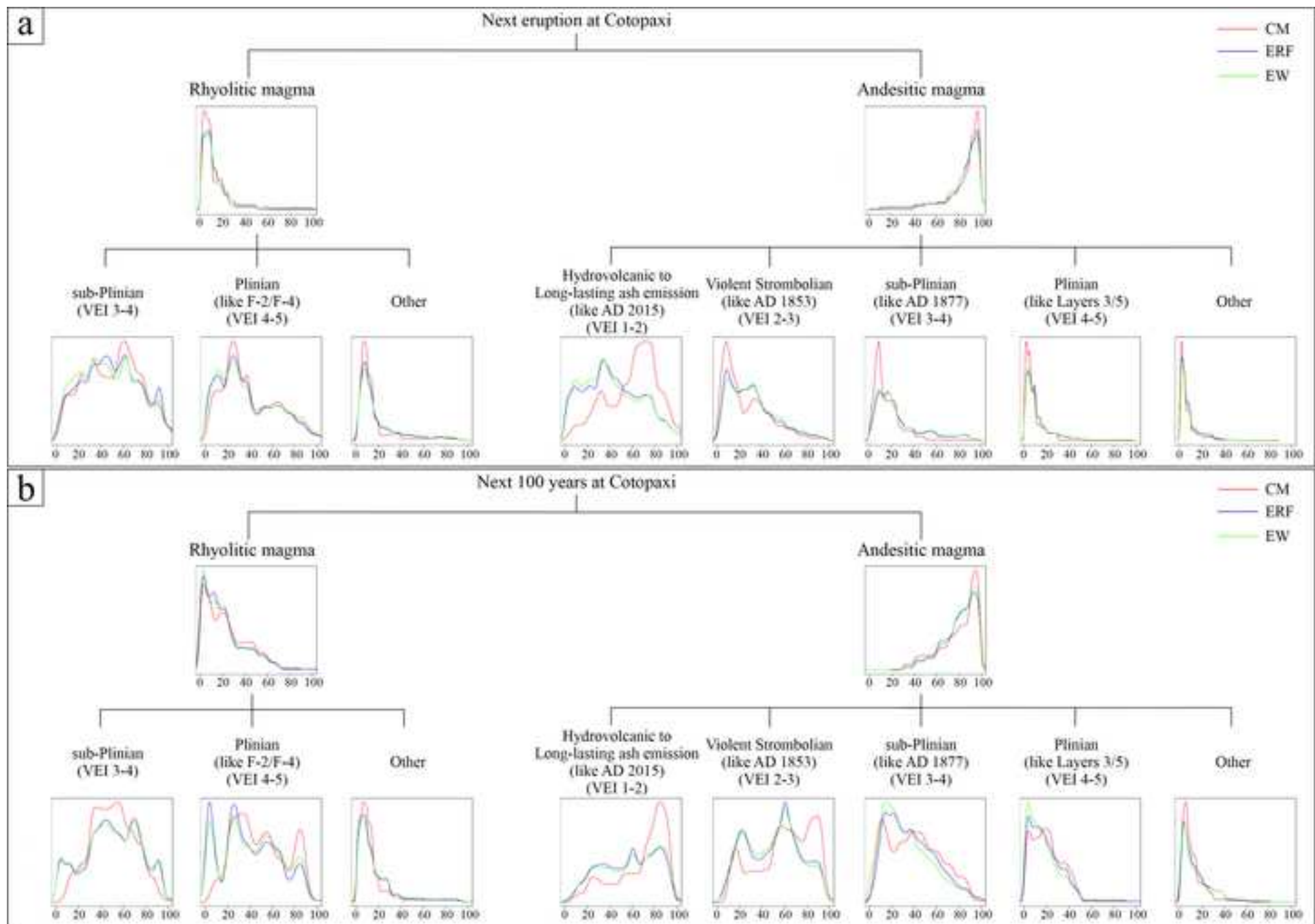
Table C1. Selected eruptions involving andesitic, dacitic and rhyolitic magmas. References: ¹Gouhier et al. (2019); ²Mastin et al. (2009); ³Risacher and Alonso (2001); ⁴Carey et al. (2010); ⁵Bonadonna et al. (2015); ⁶Durant et al. (2012).

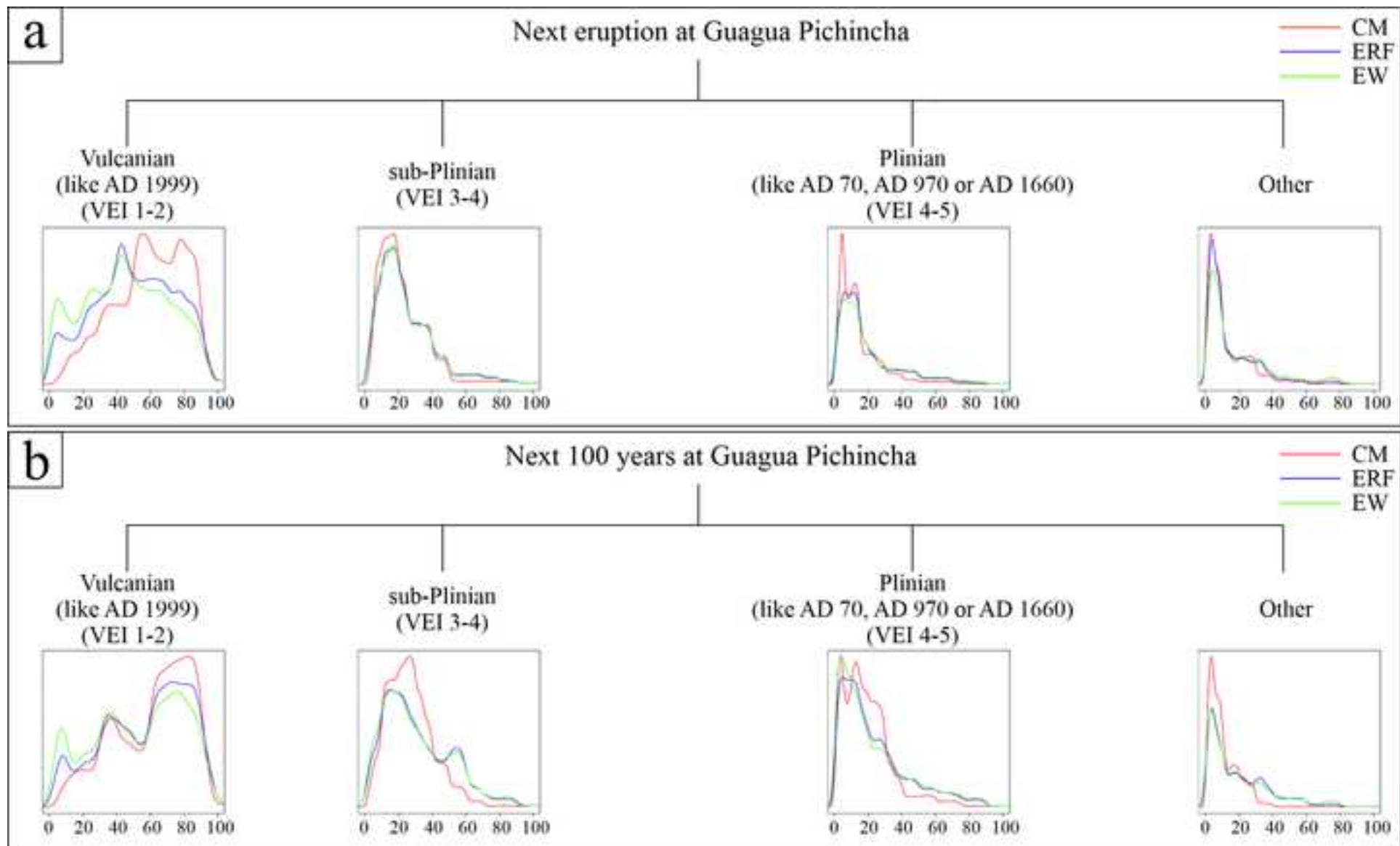


Legend

- Province boundary
- Town Building
- ▲ Volcano
- Railroad
- Major road







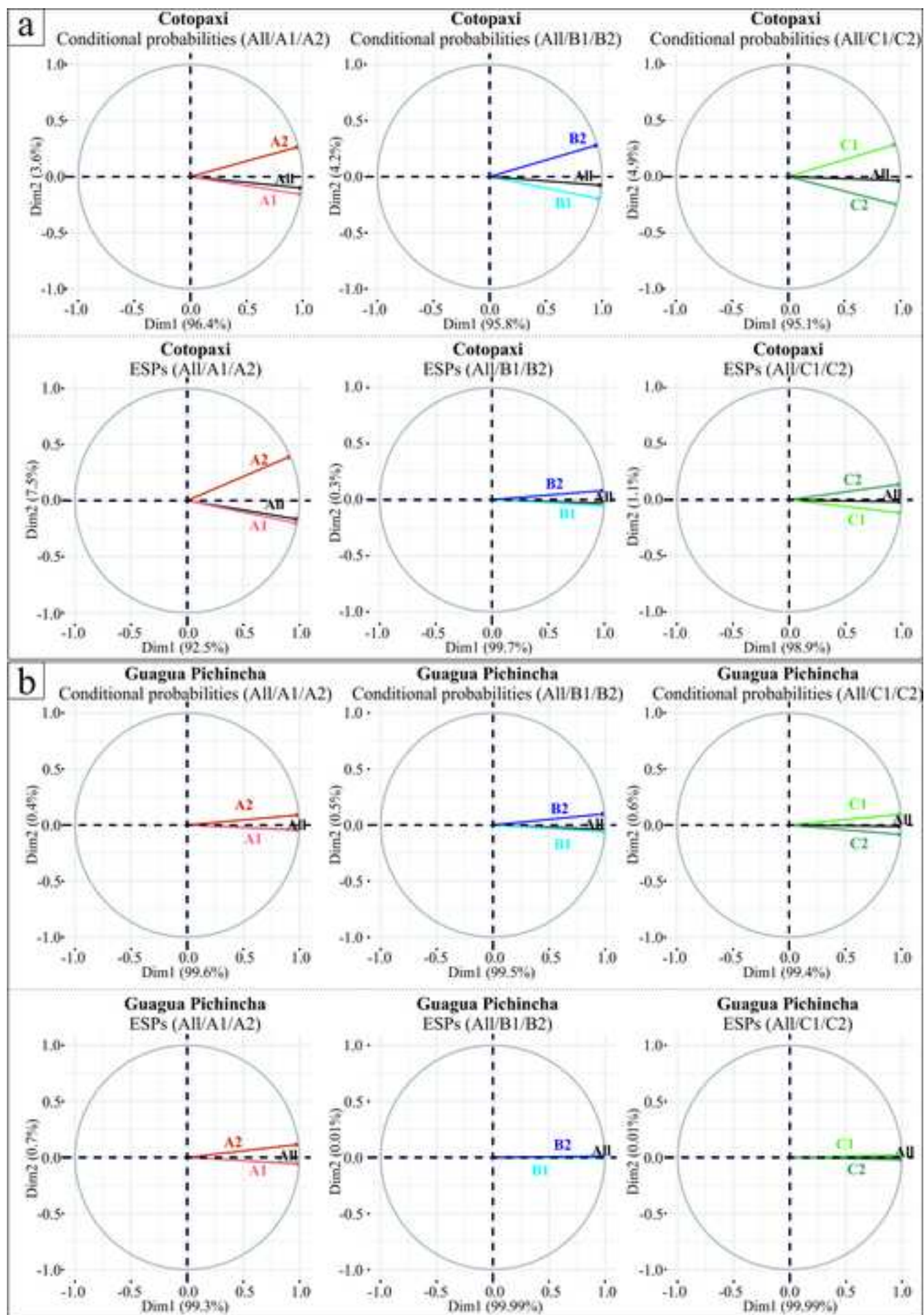


Table 1

Eruptive Cycle or Eruption Name	N° eruptions	DRE volume (km³)	Age/Date	Maximum VEI	Eruptive style(s)	Magma composition	Ref(s)
2015	1	0.0001	AD 2015	1-2	Hydrovolcanic to continuous ash emission	Andesitic	1,2,3,4
1877	1	0.02-0.06	AD 1877	4	SubPlinian		
1853	1	0.02-0.12	AD 1853	2-3	Violent Strombolian		
X/Layer 3	1	2.4	~0.9 ka	4-5	Plinian		
Y/Layer 5	1	0.5	~1.1 ka	4	Plinian		
F-4	>1	1.59-8.3	~5.8 ka	5	Plinian	Rhyolitic	1
F-2	>1	2.37-8.6	~7.8 ka	?	Plinian		

Table 2

Eruptive Cycle Name	N° eruptions	DRE volume (km3)	Age	Maximum VEI of cycle	Eruptive style(s)	Refs
1999-2001	~13	?	AD 1999-2001	0 to 1-2	~5 Vulcanian 8 Dome forming	1,2,3
Historic	4	>0.2 (of the largest eruption)	AD 1660 (of the largest eruption)	3-4	Plinian (of the largest eruption)	
X century	>1	>>0.6 (of the largest eruption)	AD 970 (of the largest eruption)	5	Plinian (of the largest eruption)	
I century	1	>0.5	AD 70	4	Plinian	

Table 3

Variable	% - 5 th /Median/95 th								
	CM			ERF			EW		
<i>% sub-Plinian Rhyolitic (NE)</i>	< 0.1	3.7	19	< 0.1	4.6	26	< 0.1	4.7	29
<i>% Plinian Rhyolitic (NE)</i>	< 0.1	2.7	15	< 0.1	3.1	20	< 0.1	3.4	24
<i>% Other type Rhyolitic (NE)</i>	< 0.1	0.9	7.5	< 0.1	1.4	12	< 0.1	1.6	14
<i>% Hydr./Ash em. Andesitic (NE)</i>	13	44	71	1.8	28	57	1.9	26	56
<i>% Violent Stromb. Andesitic (NE)</i>	1.3	15	43	1.9	18	47	2.0	19	48
<i>% sub-Plinian Andesitic (NE)</i>	0.4	9.5	33	1.2	15	45	1.1	14	44
<i>% Plinian Andesitic (NE)</i>	< 0.1	4.2	23	0.1	5.9	31	< 0.1	5.5	31
<i>% Other type Andesitic (NE)</i>	< 0.1	3.5	25	< 0.1	4.0	26	< 0.1	4.0	27
<i>% sub-Plinian Rhyolitic (N100)</i>	< 0.1	7.3	40	< 0.1	6.5	41	< 0.1	6.0	41
<i>% Plinian Rhyolitic (N100)</i>	< 0.1	6.7	41	< 0.1	4.3	36	< 0.1	4.6	37
<i>% Other type Rhyolitic (N100)</i>	< 0.1	1.5	18	< 0.1	1.4	18	< 0.1	1.5	20
<i>% Hydr./Ash em. Andesitic (N100)</i>	< 0.1	55	87	< 0.1	43	84	< 0.1	45	85
<i>% Violent Stromb. Andesitic (N100)</i>	< 0.1	47	87	< 0.1	38	81	< 0.1	38	81
<i>% sub-Plinian Andesitic (N100)</i>	< 0.1	28	75	< 0.1	25	72	< 0.1	22	73
<i>% Plinian Andesitic (N100)</i>	< 0.1	14	43	< 0.1	12	48	< 0.1	11	51
<i>% Other type Andesitic (N100)</i>	< 0.1	6.1	41	< 0.1	7.4	47	< 0.1	7.1	50

Table 4

Variable	% - 5 th /Median/95 th								
	CM			ERF			EW		
<i>% Vulcanian (NE)</i>	4.7	55	81	0.5	45	77	0.3	40	76
<i>% sub-Plinian (NE)</i>	1.8	18	55	1.0	20	60	0.3	19	60
<i>% Plinian (NE)</i>	0.3	9.9	46	0.4	13	54	0.4	14	57
<i>% Other type (NE)</i>	< 0.1	7.5	43	< 0.1	8.8	48	< 0.1	11	54
<i>% Vulcanian (N100)</i>	5.5	66	94	1.6	62	96	1.2	56	96
<i>% sub-Plinian (N100)</i>	2.1	25	63	0.9	26	83	< 0.1	26	81
<i>% Plinian (N100)</i>	1.0	17	66	< 0.1	17	82	< 0.1	16	80
<i>% Other type (N100)</i>	< 0.1	7.9	37	0.1	13	70	< 0.1	13	75

Table 5

Variable	5 th /Median/95 th								
	CM			ERF			EW		
<i>Mean duration sub-Plinian Rhyolitic (minutes)</i>	15	170	6300	13	210	4000	10	210	4100
<i>Total mass tephra sub-Plinian Rhyolitic (10⁹ kg)</i>	2.4	53	760	0.2	39	740	0.2	36	740
<i>Average plume height sub-Plinian Rhyolitic (km)</i>	5.6	16	25	2.7	17	28	2.1	17	28
<i>Mean duration Plinian Rhyolitic (minutes)</i>	27	340	13000	19	400	8900	15	330	8800
<i>Total mass tephra Plinian Rhyolitic (10⁹ kg)</i>	8.8	410	7600	0.005	450	14000	0.002	450	35000
<i>Average plume height Plinian Rhyolitic (km)</i>	10	24	40	7.8	26	40	6.5	26	40
<i>Mean duration Hyd./Ash em. Andesitic (minutes)</i>	220	41000	1200000	52	48000	800000	35	44000	710000
<i>Total mass tephra Hyd./Ash em. Andesitic (10⁹ kg)</i>	0.0001	0.8	110	0.0002	0.8	60	0.0001	0.6	58
<i>Average plume height Hyd./Ash em. Andesitic (km)</i>	0.3	3.8	14	0.2	3.2	13	0.2	3.1	13
<i>Mean duration Violent Str. Andesitic (minutes)</i>	6	42	6000	6	41	12000	6	46	32000
<i>Total mass tephra Violent Str. Andesitic (10⁹ kg)</i>	0.01	6.0	92	0.004	1.5	74	0.004	0.8	71
<i>Average plume height Violent Str. Andesitic (km)</i>	1.5	8.3	18	1.5	9.9	26	1.4	9.6	27
<i>Mean duration sub-Plinian Andesitic (minutes)</i>	9	75	9400	9	79	5500	8	73	6000
<i>Total mass tephra sub-Plinian Andesitic (10⁹ kg)</i>	1.2	34	430	0.05	21	270	0.04	18	290
<i>Average plume height sub-Plinian Andesitic (km)</i>	6.6	18	25	7.9	19	28	7.4	19	28
<i>Mean duration Plinian Andesitic (minutes)</i>	11	180	19000	12	200	11000	12	180	12000
<i>Total mass tephra Plinian Andesitic (10⁹ kg)</i>	11	220	4200	0.07	320	9900	0.04	270	14000
<i>Average plume height Plinian Andesitic (km)</i>	13	25	35	14	26	35	13	26	36

Table 6

Variable	5 th /Median/95 th								
	CM			ERF			EW		
<i>Mean duration Vulcanian (minutes)</i>	0.9	14	2300	1	17	8800	1	19	2E+05
<i>Total mass tephra Vulcanian (10⁹ kg)</i>	2E-04	1.6	71	2E-04	0.4	51	1E-04	0.3	55
<i>Average plume height Vulcanian (km)</i>	1.0	8	19	1.1	9.3	21	0.6	8.9	21
<i>Mean duration sub-Plinian (minutes)</i>	9	88	6400	8	100	4300	6	96	4300
<i>Total mass tephra sub-Plinian (10⁹ kg)</i>	0.4	28	660	0.03	18	470	0.02	13	460
<i>Average plume height sub-Plinian (km)</i>	6.9	17	25	7.9	18	27	7.4	18	28
<i>Mean duration Plinian (minutes)</i>	11	190	13000	11	240	9200	9	210	9100
<i>Total mass tephra Plinian (10⁹ kg)</i>	1.6	170	3600	0.03	170	4400	0.03	140	6800
<i>Average plume height Plinian (km)</i>	13	24	34	14	26	34	13	25	34

Eruption Cotopaxi	Mean values					
	NE (%): SUM=100			N100 (%)		
	CM	ERF	EW	CM	ERF	EW
<i>sub-Plinian Rhyolitic</i>	5.9	7.7	8.1	12	11	11
<i>Plinian Rhyolitic</i>	4.6	5.6	6.4	12	9.2	9.7
<i>Other type Rhyolitic</i>	2.0	3	3.6	4.2	4.3	4.7
<i>Hydr./Ash em. Andesitic</i>	44	28	27	51	43	44
<i>Violent Stromb. Andesitic</i>	18	21	21	45	38	38
<i>sub-Plinian Andesitic</i>	12	18	17	31	29	27
<i>Plinian Andesitic</i>	6.9	9.4	9.1	17	17	16
<i>Other type Andesitic</i>	6.8	7.2	7.5	11	13	14
Eruption Guagua Pichincha	Mean values					
	NE (%): SUM=100			N100 (%)		
	CM	ERF	EW	CM	ERF	EW
<i>Vulcanian</i>	51	44	40	60	56	52
<i>sub-Plinian</i>	22	24	24	28	32	32
<i>Plinian</i>	14	18	19	21	25	24
<i>Other type</i>	13	15	18	13	21	22

Table B2

Eruption Cotopaxi	Mean values								
	Duration (min)			Total mass fallout (10⁹ kg)			Average plume height (km)		
	CM	ERF	EW	CM	ERF	EW	CM	ERF	EW
<i>sub-Plinian Rhyolitic</i>	200	190	180	49	30	27	14	15	14
<i>Plinian Rhyolitic</i>	370	340	290	270	150	120	22	23	22
<i>Hydr./Ash em. Andesitic</i>	29000	24000	19000	0.5	0.4	0.2	3.2	2.7	2.6
<i>Violent Stromb. Andesitic</i>	73	88	120	4.0	1.1	0.9	7.3	8.3	8.1
<i>sub-Plinian Andesitic</i>	110	96	97	27	11	9.3	16	18	17
<i>Plinian Andesitic</i>	230	210	190	240	180	140	24	25	25
Eruption Guagua Pichincha	Mean values								
	Duration (min)			Total mass fallout (10⁹ kg)			Average plume height (km)		
	CM	ERF	EW	CM	ERF	EW	CM	ERF	EW
<i>Vulcanian</i>	25	30	41	0.4	0.2	0.2	6.6	7.2	6.3
<i>sub-Plinian</i>	130	110	110	24	10	7.8	16	17	17
<i>Plinian</i>	240	230	200	130	98	73	24	24	24

Table C1

Eruption	Magma type	VEI	Eruptive style	Duration (min)	Mass of fallout deposit (10 ⁹ kg)	Plume height (km)	Ref(s)
Redoubt (USA), 2009	Andesitic	-	Vulcanian	87	14	15	1
Soufrière Hills (Monsterrat, UK), 1997	Andesitic	-	Vulcanian	60	0.5	11	1
Lascar (Chile), 1993	Andesitic	-	sub-Plinian	2883	350	21	1,3
Ruapehu (New Zealand), June 1996	Andesitic	3	sub-Plinian	600	4.2	8.5	1,2
Nevado del Ruiz (Colombia), 1985	Andesitic	3	-	18	-	26	2
Spurr (USA), June 1992	Andesitic	3	sub-Plinian	264	-	14.5	1,2
Spurr (USA), August 1992	Andesitic	3	sub-Plinian	210	36	14	1,2
Spurr (USA), September 1992	Andesitic	3	sub-Plinian	216	39	14	1,2
Hekla (Iceland), 1970	Andesitic	3	-	120	-	14	2
Hekla (Iceland), 1980	Andesitic	3	-	300	-	15	2
Reventador (Ecuador), 2002	Andesitic	4	-	1320	-	17	2
Hekla (Iceland), 1947 (Brownish-grey ash)	Andesitic	4	-	30	-	28	2
Hekla (Iceland), 1947 (Brownish-black ash)	Andesitic	4	-	30	-	16	2
Soufrière St. Vincent 1902	Andesitic	4	-	150	-	14	2
El Chichón A (Mexico), 1982	Andesitic	5	-	300	-	20	2
El Chichón B and C (Mexico), 1982	Andesitic	5	Plinian	660	870	30	1,2
Hudson (Chile), 1991	Andesitic	5	Plinian	3783	3900	18	1,2
Santa Maria (Guatemala), 1902	Andesitic	6	-	1800	-	34	2
St. Helens (USA), 25 May 1980	Dacitic	3	sub-Plinian	30	42	10	2,4
St. Helens (USA), June 1980	Dacitic	3	sub-Plinian	30	45	9.6	2,4
Pinatubo (Philippines), 12 June 1991	Dacitic	3	-	38	-	17	2
St. Helens (USA), 18 May 1980	Dacitic	5	Plinian	540	630	13	2,4
Quizapu (Chile), 1932	Dacitic	6	Plinian	1080	-	28	2
Novarupta (USA), 1912 (Episode II)	Dacitic	6	Plinian	1560	4800	22	2
Novarupta (USA), 1912 (Episode III)	Dacitic	6	Plinian	600	4000	19	2
Pinatubo (Philippines), 15 June 1991	Dacitic	6	Plinian	540	5700	40	1,2
Puyehue-Cordon Caulle (Chile), June 2011 (Layers A-F)	Rhyolitic	3-4	sub-Plinian	1440	450	12	2,5
Chaitèn (Chile), May 2008 (Phases 1-4)	Rhyolitic	4	sub-Plinian	10083	171	19	2,6
Askja (Iceland), March 1875 (Units B-D)	Rhyolitic	4-5	sub-Plinian to Plinian	480	989	19	4
Novarupta (USA), 1912 (Episode I)	Rhyolitic	6	Plinian	960	4800	23	2,4